Computer Simulation Methods

University of Cambridge Part II Natural Sciences Tripos

Yue Wu

Yusuf Hamied Department of Chemistry
Lensfield Road,
Cambridge, CB2 1EW

yw628@cam.ac.uk

Acknowledgements

Nothing in these lecture notes is original. They are largely based on the notes by Prof. Rosana Collepardo, who lectured this course in 2025. Moreover, they are nowhere near accurate representations of what was actually lectured, and in particular, all errors are almost surely mine.

Contents

1 Molecular Dynamics

1.1 Integrating the Equations of Motion

A famous conclusion in classical mechanics is that the motion of three bodies under gravitational interaction has no general analytic solution in closed form. The problem will only get worse if we introduce more bodies into our systems, or we consider more complex form of the interactions. It is not uncommon for a system in physics and chemistry to have more than billions of interacting particles, so we usually have no choice but to treat their interactions numerically on a computer. The aim of *Molecular Dynamics* (MD) is to study a system by recreating it on the computer as close to nature as possible.

1.1.1 Newton's Equations of Motion

We start from the most fundamental law in classical mechanics — the Newton's equation. If we have a system of N particles, and their positions are given by $\{\mathbf{r}_i\}_{i=1}^N$ which we collectively denote as $\mathbf{r}^N$, then the interactions between the particles will be completely determined by the positions of the particles, specified by the potential

$$V = V(\mathbf{r}_1, \dots, \mathbf{r}_N) \equiv V(\mathbf{r}^N)\,. \tag{1.1}$$

The *force* $\mathbf{f}_i$ acted on particle i is the negative gradient of V, which is again a function of the configuration $\mathbf{r}^N$:

$$\mathbf{f}_i(\mathbf{r}^N) = -\boldsymbol{\nabla}_i V(\mathbf{r}^n) = -\frac{\partial V(\mathbf{r}^N)}{\partial \mathbf{r}_i}\,. \tag{1.2}$$

Then the future evolution of the system is given by the Newton's second law

$$m_i \ddot{\mathbf{r}}_i = \mathbf{f}_i(\mathbf{r}^N)\,, \tag{1.3}$$

where m_i is the mass of particle m_i. This is system of N coupled second order differential equation. Additionally, it is often useful to introduce the *momentum* of a particle. In Cartesian coordinates, the momentum of a particle is given by

$$\mathbf{p}_i = m_i \dot{\mathbf{r}}_i\,. \tag{1.4}$$

When modelling a system composed of atoms and molecules, interatomic interactions, as opposed to the forces related to chemical bonds keeping molecules together, are relatively weak. A good, and extremely common approximation for intermolecular interactions is that they are *pairwise additive.* Moreover, for atoms, these pair potentials can be assumed to be central so that they depend only on the interatomic distances. Then the total potential V can be resolved into a sum of pair potentials v_{ij} between all pairs of atoms i and j, where v_{ij} is only a function of the interatomic distance $r_{ij} \equiv \|\mathbf{r}_{ij}\| \coloneqq \|\mathbf{r}_i - \mathbf{r}_j\|$

$$V(\mathbf{r}^N) = \sum_{i=1}^{N}\sum_{j>i}^{N} v_{ij}(r_{ij})\,. \tag{1.5}$$

The sum is taken over $j > 1$ so that each pair of atoms i and j is summed exactly once. This restriction can be lifted by noting v_{ij} and v_{ji} both describes the potential between particle i and j so they should be the same, and $r_{ij} = r_{ji}$, so

$$V(\mathbf{r}^N) = \frac{1}{2}\sum_{i=1}^{N}\sum_{j\neq i}^{N} v_{ij}(r_{ij})\,. \tag{1.6}$$

The factor of a half cancels with the problem of double counting, and self interactions with $i = j$ is excluded.

If we identify the force acted on particle i by particle j is

$$\mathbf{f}_{ij} := -\frac{\partial v_{ij}}{\partial \mathbf{r}_i}\,, \tag{1.7}$$

then it is easy to show that the total force acted on particle i is the sum of the forces acted by all other particles using the form of potential given by (1.6)

$$\begin{aligned}\mathbf{f}_i &= -\frac{\partial V}{\partial \mathbf{r}_i}\\ &= -\frac{1}{2}\sum_{j\neq i}^{N}\left(\frac{\partial v_{ij}(r_{ij})}{\partial \mathbf{r}_i} + \frac{\partial v_{ji}(r_{ji})}{\partial \mathbf{r}_i}\right)\\ &= -\sum_{j\neq i}^{N}\frac{\partial v_{ij}(r_{ij})}{\partial \mathbf{r}_i} = \sum_{j\neq i}^{N}\mathbf{f}_{ij}\,. \end{aligned}\tag{1.8}$$

It is also not difficult to should that the pair forces satisfy the Newton's third law

$$\mathbf{f}_{ij} = -\mathbf{f}_{ji}\,. \tag{1.9}$$

1.1.2 Properties of Classical Dynamics

Energy Conservation

A fundamental property of mechanical systems, for pair or many-body interactions, provided that they can be derived from a potential invariant in time, is that the total energy is conserved during the motion. The total energy is sum of the potential energy V and the kinetic energy K defined by

$$K = \sum_{i=1}^{N}\frac{1}{2}m_i\dot{\mathbf{r}}_i^2\,. \tag{1.10}$$

We define the *Hamiltonian* of a system to be

$$H(\mathbf{r}^N, \dot{\mathbf{r}}^N, t) := K + V = \sum_{i=1}^{N}\frac{1}{2}m_i\dot{r}_i^2 + V(\mathbf{r}^N, t)\,, \tag{1.11}$$

For our purposes, it is just another way of saying the total energy of the system.[1] In our cases, the potential V and hence the whole Hamiltonian has no explicit time dependence, meaning t does not appear explicitly in the expression of both K and V, although both $\mathbf{r}$ and $\dot{\mathbf{r}}$ evolve in time. If this is the case, then the Hamiltonian (energy) does not change in time. This is the conservation of energy.

Theorem 1.1 (Energy Conservation). If $H(\mathbf{r}_i, \dot{\mathbf{r}}_i, t)$ has no explicit time dependence,

$$\frac{\partial H}{\partial t} = 0\,, \tag{1.13}$$

then H is a constant of motion,

$$\frac{\mathrm{d}H}{\mathrm{d}t} = 0\,. \tag{1.14}$$

[1] Formally in classical mechanics, the Hamiltonian is defined as the Legendre transform of the Lagrangian, by

$$H = \sum_{i=1}^{n} p_i\dot{q}_i - L(q_i, \dot{q}_i, t)\,. \tag{1.12}$$

p_i is shown as the *conjugated momentum* of the *generalised coordinate* q_i. Since the generalised coordinate is not necessarily the Cartesian coordinates (e.g. spherical, or even non-orthogonal), H may not be the energy.

Proof. By chain rule,

$$
\begin{aligned}
\frac{\mathrm{d}H}{\mathrm{d}t} &= \frac{\partial H}{\partial t} + \sum_{i=1}^{N} \frac{\partial H}{\partial \mathbf{r}_i}\frac{\partial \mathbf{r}_i}{\partial t} + \sum_{i=1}^{N} \frac{\partial H}{\partial \dot{\mathbf{r}}_i}\frac{\partial \dot{\mathbf{r}}_i}{\partial t} && (1.15)\\
&= 0 + \sum_{i=1}^{N} \frac{\partial V}{\partial \mathbf{r}_i} \cdot \dot{\mathbf{r}}_i + \sum_{i=1}^{N} m_i \dot{\mathbf{r}}_i \cdot \ddot{\mathbf{r}}_i && (1.16)\\
&= \sum_{i=1}^{N} \dot{\mathbf{r}}_i \cdot (\mathbf{f}_i - m_i \ddot{\mathbf{r}}_i) = 0 && (1.17)
\end{aligned}
$$

from Newton's second law. □

Since the Hamiltonian is not explicitly dependent on time, the system has time-translational symmetry, meaning that we start the system at time t and at time $t + \delta t$, the system will evolve in the same way. This result of a continuous symmetry of the system leading to a conserved quantity is an example of the Noether's theorem, which is arguably the most beautiful and profound result in physics. We will briefly introduce this result in section A.

The conservation of energy is fundamental in the derivation of the equilibrium ensembles in statistical mechanics. It can also be applied as a very powerful test of the stability of a numerical scheme for the integration of the equations of motion. We will repeatedly return to this point.

Time Reversal Symmetry

Another feature of Newtonian dynamics that plays a role both in the theory of statistical mechanics and in the practice of the development of molecular dynamics algorithms is *time reversal symmetry.* This states that if we reverse all velocities at time t while keeping the positions the same, then the system will retrace its trajectory back into the past. We introduce the notation

$$\mathbf{r}^N(t \mid \mathbf{r}_0^N, \mathbf{p}_0^N) \tag{1.18}$$

to be $\mathbf{r}^N$ under the initial condition $\mathbf{r}^N(0) = \mathbf{r}_0^N$ and $\mathbf{p}^N(0) = \mathbf{p}_0^N$. Then time reversal symmetry implies the relations

$$
\begin{aligned}
\mathbf{r}^N(t \mid \mathbf{r}^N(0), -\mathbf{p}^N(0)) &= \mathbf{r}^N(-t \mid \mathbf{r}^N(0), \mathbf{p}^N(0))\,, && (1.19)\\
\mathbf{p}^N(t \mid \mathbf{r}^N(0), -\mathbf{p}^N(0)) &= -\mathbf{p}^N(-t \mid \mathbf{r}^N(0), \mathbf{p}^N(0))\,. && (1.20)
\end{aligned}
$$

1.1.3 The Euler's Algorithm

Molecular dynamics methods are iterative numerical schemes for solving the equations of motion of the system. The first step is to discretise the time into small intervals, and we assume each interval has equal length δt. Then the evolution of the system is then described by the series of coordinates and velocities

$$
\begin{aligned}
&\mathbf{r}^N(t_0) \equiv \mathbf{r}^N(0), \dots, \mathbf{r}^N(t_{m-1}) \equiv \mathbf{r}^N(t_m - \delta t), \mathbf{r}^N(t_m), \mathbf{r}^N(t_{m+1}) \equiv \mathbf{r}^N(t_m + \delta t), \dots && (1.21)\\
&\dot{\mathbf{r}}^N(t_0) \equiv \dot{\mathbf{r}}^N(0), \dots, \dot{\mathbf{r}}^N(t_{m-1}) \equiv \dot{\mathbf{r}}^N(t_m - \delta t), \dot{\mathbf{r}}^N(t_m), \dot{\mathbf{r}}^N(t_{m+1}) \equiv \dot{\mathbf{r}}^N(t_m + \delta t), \dots && (1.22)
\end{aligned}
$$

The Schemes we will discuss all use the Cartesian coordinates.

The most fundamental integrator in molecular dynamics is the *Euler's algorithm.* It approximates the position of the molecule at time $t + \delta t$ by a Taylor series about t truncated at $O(\delta t^2)$

$$\begin{aligned} \mathbf{r}_i(t+\delta t) &= \mathbf{r}_i(t) + \dot{\mathbf{r}}(t)\delta t + \frac{1}{2}\ddot{\mathbf{r}}(t)\delta t^2 + O(\delta t^3) \\ &= \mathbf{r}_i(t) + \delta t \mathbf{v}_i(t) + \frac{\delta t^2}{2m_i}\mathbf{f}_i(t) + O(\delta t^3)\,. \end{aligned} \tag{1.23}$$

Similarly one can obtain an expansion for $\mathbf{v}_i(t + \delta t)$

$$\mathbf{v}_i(t+\delta t) = \mathbf{v}_i(t) + \frac{\delta t}{m_i}\mathbf{f}_i(t) + (\delta t^3)\,. \tag{1.24}$$

Having an expression of $\mathbf{f}_i$, which can be worked out from the potential V, we can perform this process iteratively.

Algorithm 1.2 (Euler's Algorithm).

$$\mathbf{r}_i(t+\delta t) = \mathbf{r}_i(t) + \delta t \mathbf{v}_i(t) + \frac{\delta t^2}{2m_i}\mathbf{f}_i(t) \tag{1.25}$$

$$\mathbf{v}_i(t+\delta t) = \mathbf{v}_i(t) + \frac{\delta t}{m_i}\mathbf{f}_i(t)\,. \tag{1.26}$$

The error is $O(\delta t^3)$.

The Euler's algorithm is simple, but it has a huge drawback — it is simply not accurate enough.

To illustrate this, we calculated the equation of motion of a standard Harmonic oscillator, with Hamiltonian

$$H = \frac{1}{2}v^2 + \frac{1}{2}x^2 \tag{1.27}$$

and initial conditions $x_0 = 0$ and $v_0 = 1$. The results are plotted in figure 1. The exact solution is a sine wave

$$x(t) = \sin t\,. \tag{1.28}$$

We can see that the Euler's solution quickly diverges from the exact solution as amplitude of oscillation quickly grows larger and larger. The Euler's algorithm has several problems, making it very limited in current practical use:

- The solution is not time reversible.
- *Liouville theorem* states that the volume of a a set in the phase space should conserve as it evolve with time. In Euler's algorithm, the volume in the phase space is not conserved.
- The system is susceptible to energy drift. As we can see in the plot, the energy drifts exponentially fast.

This suggests that we need a more accurate algorithm.

1.1.4 Verlet Algorithm

An obvious thing to do to improve the Euler's algorithm is to include more terms in the Taylor expansions. If we truncate the expansion of $\mathbf{x}(t + \delta t)$ at $O(\delta t^3)$, we get

$$\mathbf{r}_i(t+\delta t) = \mathbf{r}_i(t) + \delta t \mathbf{v}_i(t) + \frac{\delta t^2}{2m_i}\mathbf{f}_i(t) + \frac{\delta t^3}{6}\mathbf{b}_i(t) + O(\delta t^4)\,, \tag{1.29}$$

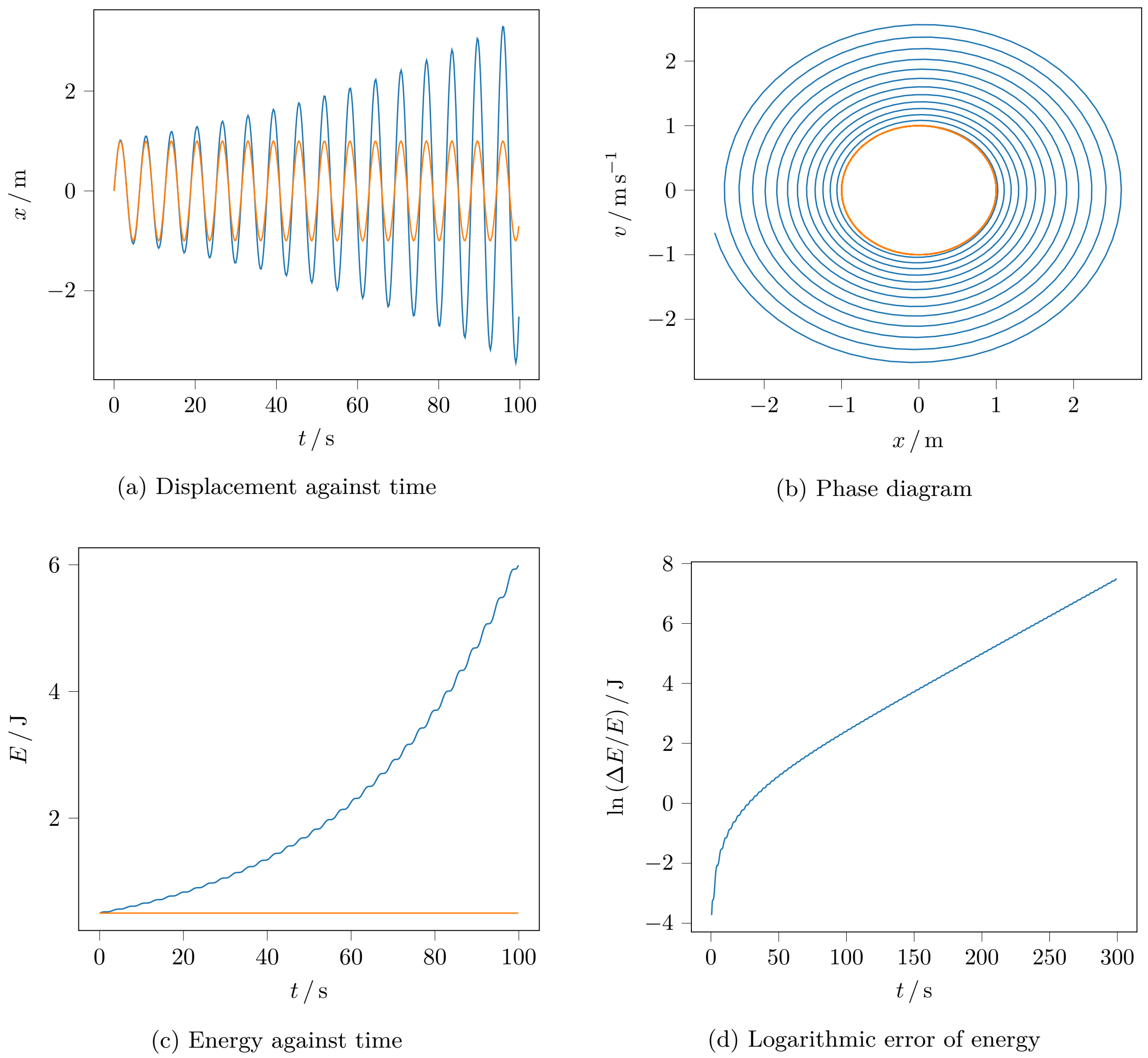

(a) Displacement against time

(b) Phase diagram

(c) Energy against time

(d) Logarithmic error of energy

Figure 1: The motion of a harmonic oscillator solved by Euler's method (blue) and the exact solution (orange). The step length in Euler's method is set to be $\delta t = 0.05\,\mathrm{s}$.

where $\mathbf{b}_i \coloneqq \dddot{\mathbf{r}}_i$ is the third derivative of position. But this leads to a problem — it is not easy to evaluate this third derivative. But the trick is we don't have to evaluate it. If we expand the position backward in time, we get

$$\mathbf{r}_i(t-\delta t) = \mathbf{r}_i(t) - \delta t\mathbf{v}_i(t) + \frac{\delta t^2}{2m_i}\mathbf{f}_i(t) - \frac{\delta t^3}{6}\mathbf{b}_i(t) + O(\delta t^4)\,. \tag{1.30}$$

Now if we add these two expressions together, the third derivatives nicely cancel out and we are left with

$$\mathbf{r}_i(t+\delta t) = 2\mathbf{r}_i(t) - \mathbf{r}_i(t-\delta t) + \frac{\delta t^2}{m_i}\mathbf{f}_i(t) + O(\delta t^4)\,. \tag{1.31}$$

Now this expression is accurate to $O(\delta t^3)$, and we don't even need to evaluate the velocities $\mathbf{v}(t)$ if we are only interested in time.

However, in most cases, the velocities still tell us valuable informations. To calculate it, we can subtract the two expansions forward and backward in time and get

$$\mathbf{v}_i(t) = \frac{1}{2\delta t}[\mathbf{r}_i(t+\delta t) - \mathbf{r}_i(t-\delta t)] + O(\delta t^3)\,. \tag{1.32}$$

Algorithm 1.3 (Verlet Algorithm).

$$\mathbf{r}_i(t+\delta t) = 2\mathbf{r}_i(t) - \mathbf{r}_i(t-\delta t) + \frac{\delta t^2}{m_i}\mathbf{f}_i(t) \tag{1.33}$$

$$\mathbf{v}_i(t) = \frac{1}{2\delta t}[\mathbf{r}_i(t+\delta t) - \mathbf{r}_i(t-\delta t)]\,. \tag{1.34}$$

The error of displacement is $O(\delta t^4)$ and that of velocity is $O(\delta t^3)$.

However, to calculate $\mathbf{v}(t)$, you need the knowledge of position at $t+\delta t$, i.e. the velocity update in the Verlet algorithm is one step behind the position update. This is not a problem for propagating position because, assuming that the forces are not dependent on velocity, information on $\mathbf{v}_i(t)$ is not needed in (equation (1.33)). Still, this may be inconvenient for the determination of velocity-dependent quantities or for the algorithms which manipulate the velocity during dynamics. The position and velocity update can be brought in the same step by a reformulation of the Verlet scheme, called *velocity Verlet.* The prediction for position is now simply obtained from the Taylor expansion, again keeping to the second order

$$\mathbf{r}_i(t+\delta t) = \mathbf{r}_i(t) + \delta t\mathbf{v}_i(t) + \frac{\delta t^2}{2m_i}\mathbf{f}_i(t) + O(\delta t^3)\,. \tag{1.35}$$

For the advanced position obtained this way we compute the force at time $t+\delta t$

$$\mathbf{f}_i(t+\delta t) = \mathbf{f}_i(\{\mathbf{r}_j(t+\delta t)\}) = \mathbf{f}_i\left(\left\{\mathbf{r}_i(t) + \delta t\mathbf{v}_i(t) + \frac{\delta t^2}{2m_i}\mathbf{f}_i(t)\right\}\right)\,, \tag{1.36}$$

in which all particles have proceeded to their positions at $t+\delta t$. Substituting this expression into the Taylor expansion of $\mathbf{r}_i(t)$ about $t+\delta t$ backward in take, we obtain

$$\mathbf{r}_i(\mathbf{t}) = \mathbf{r}_i(t+\delta t) - \delta t\mathbf{v}_i(t+\delta t) + \frac{\delta t^2}{2m_i}\mathbf{f}_i(t+\delta t) + O(\delta t^3)\,. \tag{1.37}$$

Adding this to the forward expansion (1.35) gives the prediction of velocity

$$\mathbf{v}_i(t+\delta t) = \mathbf{v}_i(t) + \frac{\delta t}{2m_i}[\mathbf{f}_i(t) + \mathbf{f}_i(t+\delta t)] + O(\delta t^3)\,. \tag{1.38}$$

Algorithm 1.4 (Velocity Verlet Algorithm).

$$\mathbf{r}_i(t+\delta t) = \mathbf{r}_i(t) + \delta t\mathbf{v}_i(t) + \frac{\delta t^2}{2m_i}\mathbf{f}_i(t) \tag{1.39}$$

$$\mathbf{v}_i(t+\delta t) = \mathbf{v}_i(t) + \frac{\delta t}{2m_i}[\mathbf{f}_i(t) + \mathbf{f}_i(t+\delta t)]\,. \tag{1.40}$$

The velocity Verlet looks rather different than the Verlet algorithm, especially the $O(\delta t^3)$ error terms when we derive it look concerning. However, we can show that these two algorithms are equivalent. We can show this by rewriting the velocity Verlet prediction of the position.

Proposition 1.5. The velocity Verlet algorithm is equivalent to the Verlet algorithm.

Proof. If we subtract the $t-\delta t \to t$ prediction for the position from the $t \to t+\delta t$ prediction in the velocity Verlet algorithm, we find

$$\mathbf{r}_i(t+\delta t) - \mathbf{r}_i(t) = \mathbf{r}_i(t) - \mathbf{r}_i(t-\delta t) + \delta t[\mathbf{v}_i(t) - \mathbf{v}_i(t-\delta t)] + \frac{\delta t^2}{2m_i}[\mathbf{f}_i(t) - \mathbf{f}_i(t-\delta t)]\,. \tag{1.41}$$

The $t-\delta t \to t$ update for the velocity is

$$\mathbf{v}_i(t) = \mathbf{v}_i(t-\delta t) + \frac{\delta t}{2m_i}[\mathbf{f}_i(t-\delta t) + \mathbf{f}_i]\,. \tag{1.42}$$

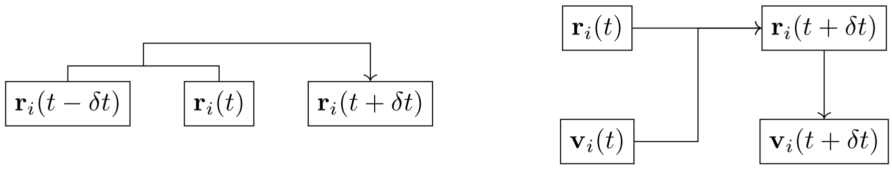
$\mathbf{r}_i(t-\delta t)$
$\mathbf{r}_i(t)$
$\mathbf{r}_i(t+\delta t)$
$\mathbf{r}_i(t)$
$\mathbf{r}_i(t+\delta t)$
$\mathbf{v}_i(t)$
$\mathbf{v}_i(t+\delta t)$

Verlet algorithm

velocity Verlet algorithm

Figure 2: Schemes of Verlet and velocity Verlet algorithms.

If we substitute this into (1.41), we get

$$\mathbf{r}_i(t+\delta t) = 2\mathbf{r}_i(t) - \mathbf{r}_i(t-\delta t) + \frac{\delta t^2}{m_i}\mathbf{f}_i(t)\,. \tag{1.43}$$

The velocity Verlet algorithm gives the same prediction with the Verlet algorithm. □

Now let's examine the accuracy of Verlet's algorithm using harmonic oscillator.

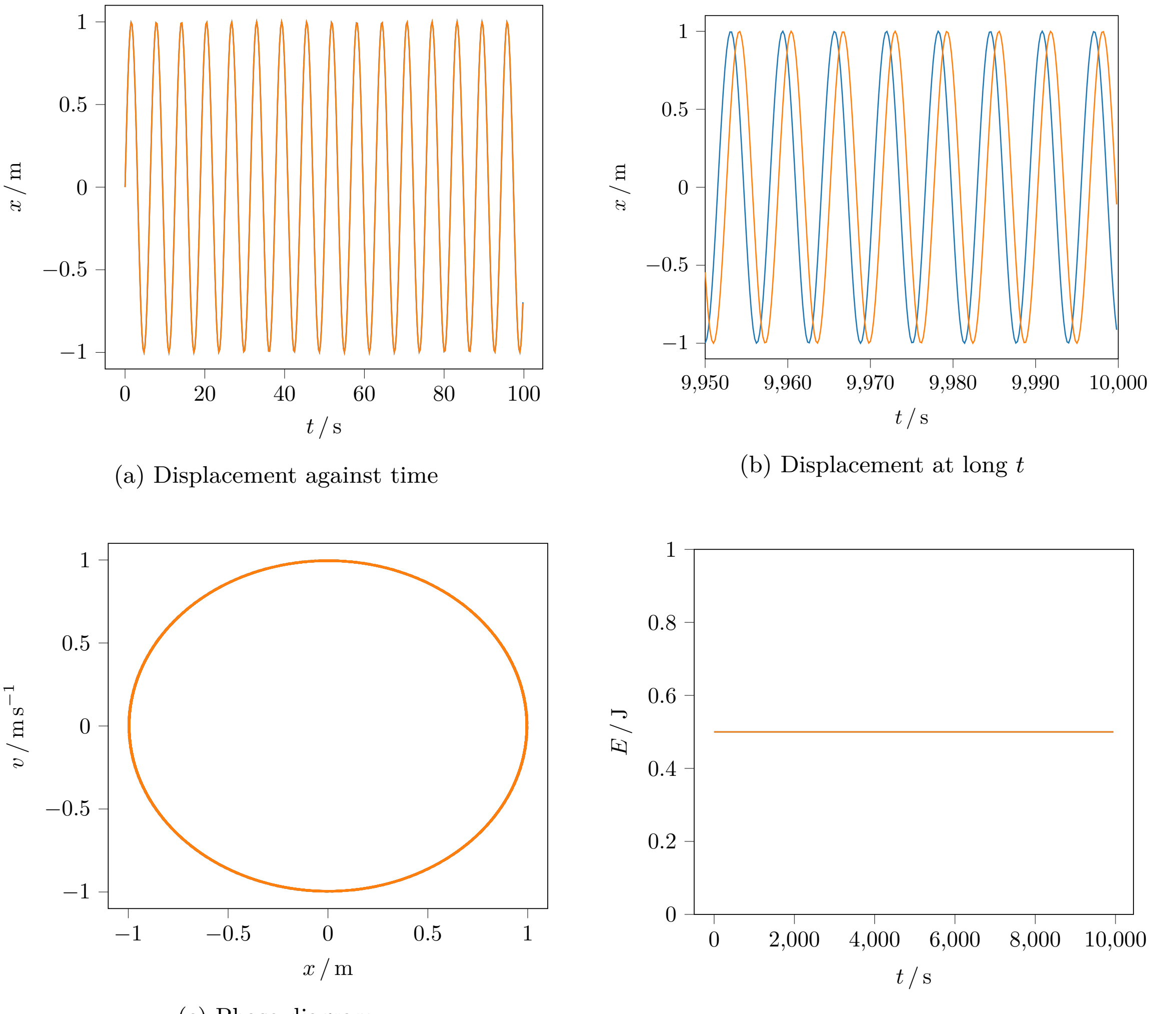

(a) Displacement against time

(b) Displacement at long t

(c) Phase diagram

(d) Energy against time

Figure 3: The motion of a harmonic oscillator solved by Verlet algorithm (blue) and the exact solution (orange). The step length in Verlet's method is also $\delta t = 0.05\,\mathrm{s}$.

We can see that the Verlet algorithm is very accurate. Although the displacements start to deviate from the exact displacement and a very long time, the energy and the volume in the phase space is always conserved.

1.1.5 Why use the Verlet Algorithm? (Non-examinable)

While there are algorithms with better short time accuracy than the Verlet algorithm, the overwhelming majority of condensed matter molecular dynamics simulations is based on just the Verlet algorithm. There are a number of reasons for its popularity.

(i) The Verlet algorithm is simple and only depends on forces. No higher derivatives of the energy is needed. This is important because the force evaluation is the most CPU time consuming in MD simulations of interacting many-particle systems. Computation of higher derivatives of energy will increase computational costs substantially. Although the algorithms using force derivatives are more accurate, this gain is actually relatively minor. Because of the chaotic nature of the motion in many-particle systems, the particles rapidly deviate from the "true" trajectories. This is known as *Lyapunov instability*: trajectories that differ slightly in initial conditions will diverge exponentially in time. If we denote $\mathbf{r}(t) = \mathbf{r}(t \mid \mathbf{r}_0, \mathbf{p}_0)$ and $\mathbf{r}'(t) = \mathbf{r}(t \mid \mathbf{r}_0, \mathbf{p}_0 + \epsilon)$, then

$$|\mathbf{r}(t) - \mathbf{r}'(t)| \sim \epsilon \exp(\lambda t)\,, \tag{1.44}$$

where λ is the *Lyapunov exponent.* This can be seen if we plot the logarithmic error of displacement against time, where the upper bound of the plot is a straight line with gradient λ.

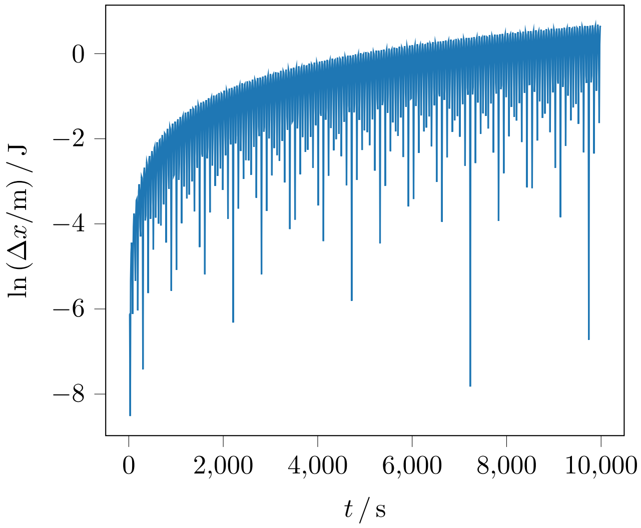

Figure 4: Logarithmic error of displacement of a harmonic oscillator using Verlet algorithm.

Having an exponentially growing error many seems horrible, but it is actually not as big a problem as it seems!

Theorem 1.6 (Shadowing theorem). Every numerical trajectory will be uniformly close to some true trajectory with slightly altered initial position. In other words, a numerical trajectory is "shadowed" by a true one.

This strong molecular chaos is ultimately the justification of methods of statistical mechanics.

(ii) Even though only using forces, the Verlet algorithm is correct up to and including $O(\delta t^3)$.

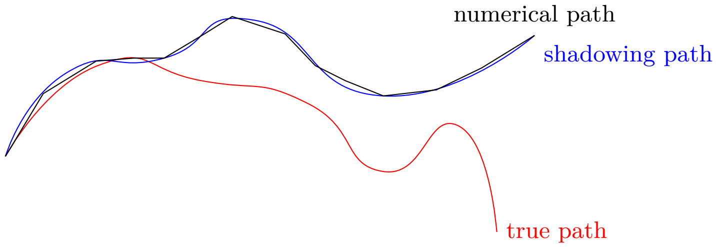

(iii) The Verlet algorithm is explicitly time reversible and, even though the trajectory relatively quickly diverges substantially from the true trajectory, the energy is conserved over an extremely long period of time. Moreover, the Verlet algorithm rigorously conserves the normalisation of an ensemble probability distribution of points in phase space. In more advanced language, the Verlet integrator is said to be *symplectic*. These formal properties contribute to the superior long time stability of the Verlet algorithm.

For example, as we will discuss later, energy is the defining quantity for the microcanonical ensemble, since, for chaotic systems, there are no constrains on the regions trajectories can reach in phase space other than that they are confined to the hypersurface of constant energy. Energy conservation, together with norm conservation are therefore necessary conditions for thermodynamic stability, and ultimately for a proper definition of temperature. Long time stability is particularly important for the simulation of liquids which are stabilised by finite temperature dynamical fluctuations.

1.2 Connection to Equilibrium Statistical Mechanics

1.2.1 The Microcanonical Ensemble

So far, we have studied systems using Newtonian dynamics, in which the energy is naturally conserved if the system is closed. This corresponds to a microcanonical ensemble. For each observable A of the system, there is a corresponding *phase function* $\mathcal{A}(\mathbf{r}^N, \mathbf{p}^N)$ telling us the value of A given a state $(\mathbf{r}^N, \mathbf{p}^N)$ of the system. Then the ensemble average of the system is given by

$$\langle A \rangle_{NVE} = \int \mathrm{d}^{3N}\mathbf{r}^N \, \mathrm{d}^{3N}\mathbf{p}^N \, \rho_{NVE}(\mathbf{r}^N, \mathbf{p}^N)\mathcal{A}(\mathbf{r}^N, \mathbf{p}^N) \,, \tag{1.45}$$

where $\rho_{NVE}(\mathbf{r}^N, \mathbf{p}^N)$ is the *microcanonical phase-space distribution function* restricting the manifold of accessible phase points $(\mathbf{r}^N, \mathbf{p}^N)$ to a hypersurface of constant energy E only, given by

$$\rho_{NVE}(\mathbf{r}^N, \mathbf{p}^N) = \frac{f(N)}{\Omega_N} \delta(\mathcal{H}(\mathbf{r}^N, \mathbf{p}^N) - E) \,. \tag{1.46}$$

The phase function $\mathcal{H}(\mathbf{r}^N, \mathbf{p}^N)$ is the Hamiltonian, $f(N)$ is some function of the number of particles accounting for their indistinguishability, and Ω_N is the microcanonical partition function given by

$$\Omega_N = f(N) \int \mathrm{d}^{3N}\mathbf{r}^N \, \mathrm{d}^{3N}\mathbf{p}^N \, \delta(\mathcal{H}(\mathbf{r}^N, \mathbf{p}^N) - E) \,. \tag{1.47}$$

The factors $f(N)$ in the above expression can be omitted if we are only interested in mechanical observable averages over the ensemble distributions using ρ_{NVE}, but it becomes crucial if we want to give the normalisation factor Ω_N a thermodynamical interpretation when calculating entropy, free energy *etc.*

1.2.2 The Ergodic Principle and Time Averages

The above thermodynamic average of a quantity require us to evaluate it over the whole hypersurface of constant energy $\mathcal{H}(\mathbf{r}^N, \mathbf{p}^N)$ in the phase space — it is difficult to do this in a computer simulation. However, we know that the state of a deterministic NVE system also evolve on this hypersurface of constant energy with time, with trajectory $(\mathbf{r}^N(t), \mathbf{p}^N(t))$. This allows us to determine how the physical observable A evolve along a certain trajectory as a function of time

$$A(t) \equiv \mathcal{A}(\mathbf{r}^N(t), \mathbf{p}^N(t))\,. \tag{1.48}$$

Now we are going to evoke some hypothesis.

Hypothesis 1.7 (Ergodic Hypothesis). Over a long enough period of time, the time spent by a system in some region of the phase space of microstates with the same energy is proportional to the volume of this region, i.e., that all accessible microstates are equiprobable over a long period of time.

This means that if we let our system evolve for a long period of time, then it will go over the whole subset of the phase space that it is allowed to go to — it is not saying that it will travel to every single point in the hypersurface of constant energy, which is impossible for a finite amount of time. What we are saying is that the system is sampling through a large enough portion of the phase space, so that the time average of the quantity $A(t)$ is essentially the ensemble average $\langle A \rangle_{NVT}$. We are replacing the ensemble average with a time average from a very long trajectory.

$$\langle A \rangle_{NVE} = \lim_{\tau\to\infty} \overline{A}_\tau = \lim_{\tau\to\infty} \frac{1}{\tau}\int_0^\tau \mathrm{d}t\, \mathcal{A}(\mathbf{r}^N(t), \mathbf{p}^N(t))\,. \tag{1.49}$$

In molecular dynamics computer simulation, we can only approximate a discrete path of time interval δt over a finite amount of time $\tau = M\delta t$. We then need to replace the above integral by a sum.

$$\langle A \rangle_\tau \approx \frac{1}{M}\sum_{m=1}^{M} \mathcal{A}(\mathbf{r}^N(t_m), \mathbf{p}^N(t_m))\,. \tag{1.50}$$

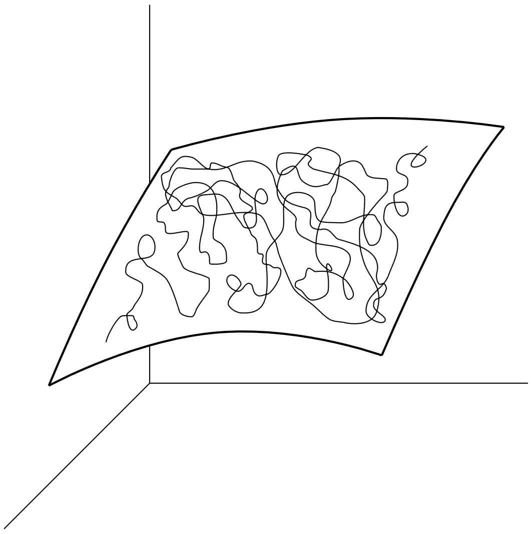

Figure 5: By the ergodic hypothesis, a trajectory will sample enough points on the whole hypersurface of constant energy such that the time average is a very good approximation to the ensemble average.

1.2.3 The Canonical Ensemble

Real world systems are hardly ever isolated. The least they do is to exchange energy with the environment. The states of such a system in equilibrium with a thermal reservoir of temperature T

are distributed according to the canonical ensemble

$$\rho_{NVT}(\mathbf{r}^N, \mathbf{p}^N) = \frac{f(N)}{Q(N)} \exp\left(-\frac{\mathcal{H}(\mathbf{r}^N, \mathbf{p}^N)}{k_B T}\right) , \tag{1.51}$$

where Q is the canonical partition function

$$Q_N = f(N) \int \mathrm{d}^{3N}\mathbf{r}^N \, \mathrm{d}^{3N}\, \mathbf{p}^N \exp\left(-\frac{\mathcal{H}(\mathbf{r}^N, \mathbf{p}^N)}{k_B T}\right) . \tag{1.52}$$

Canonical expectation values of observables are exponentially weighted averages over all points in phase space

$$\langle A \rangle_{NVT} = \int \mathrm{d}^{3N}\mathbf{r}^N \, \mathrm{d}^{3N}\mathbf{p}^N \, \rho_{NVT}(\mathbf{r}^N, \mathbf{p}^N)\mathcal{A}(\mathbf{r}^N, \mathbf{p}^N) \tag{1.53}$$

$$= \frac{f(N)}{Q_N} \int \mathrm{d}^{3N}\mathbf{r}^N \, \mathrm{d}^{3N}\mathbf{p}^N \, \mathcal{A}(\mathbf{r}^N, \mathbf{p}^N) \exp(-\beta\mathcal{H}(\mathbf{r}^N, \mathbf{p}^N)) . \tag{1.54}$$

By taking the classical limit of the quantum canonical ensemble, the expression for the factor $f(N)$ can evaluated. If all N particles are identical, then it is

$$f(N) = \frac{1}{h^{3N} N!} . \tag{1.55}$$

The canonical partition function Q_N and microcanonical partition function Ω_N have all taken this into account. Their interpretation is suggested by considering the dimension of h, which is equal to that of position times momentum. $f(N)$ is therefore a very small reciprocal space volume which makes the canonical/microcanonical partition function dimensionless. Planck's constant therefore acts as a measure of the phase space metric and Q_N is interpreted as the effective number of accessible states at temperature T. The $N!$ factor takes account of the indistinguishability of the particles. It can be viewed as correcting for over-counting in the classical ensemble where permuting the position and momentum of a pair of particles would lead to a different but equivalent state (point) $(\mathbf{r}^N, \mathbf{p}^N)$ in the phase space. Similarly Ω_N is also the number of accessible states, except that in microcanonical ensemble it is restricted to the hypersurface of constant energy in the phase space (a manifold of dimension $6N-1$). A mathematically more correct way of thinking the microcanonical partition function is that for a given infinitesimal change in energy $\mathrm{d}E$, the quantity $\Omega_N \mathrm{d}E$ gives the effective number of states contained in the volume between hypersurfaces with energy E and $E + \mathrm{d}E$.

Ω_N and Q_N are related to two very important thermodynamic quantities, namely the Boltzmann entropy

$$S = k_B \ln \Omega_N \tag{1.56}$$

and the Helmholtz free energy

$$A = -k_B T \ln Q_N . \tag{1.57}$$

They are the central relations linking statistical mechanics to thermodynamics. The factor $f(N)$ plays a crucial role in this identification. The founding fathers of statistical mechanics arrived at these results without the help of quantum mechanics — arguments concerning the additivity of entropy of mixing and similar considerations led them to postulate the form of the N dependence.

1.2.4 The Configuration Integral

It turns out that the kinetic energy is a rather trivial quantity in classical statistical thermodynamics.

Theorem 1.8 (Equipartition theorem). The average kinetic energy per particle is

$$\langle K \rangle = \frac{d}{2} k_B T , \tag{1.58}$$

where d is the dimension of the system.

This result is independent of the interaction potential or the mass. The origin of this is because the kinetic energy always takes the same form

$$\mathcal{K}(\mathbf{p}^N) = \frac{1}{2}\sum_{i=1}^{N}\frac{\mathbf{p}_i^2}{2m}\,. \tag{1.59}$$

When we evaluate the partition function, we can separate the Hamiltonian into a kinetic and a potential part, and the integral over the kinetic part will always be the same.

$$\begin{aligned}Q_N &= f(N)\int \mathrm{d}^{3N}\mathbf{p}^N\,\mathrm{d}^{3N}\mathbf{r}^N\,\exp(-\beta\mathcal{H}(\mathbf{r}^N,\mathbf{p}^N))\\ &= f(N)\int \mathrm{d}^{3N}\mathbf{p}^N\,\exp(-\beta\mathcal{K}(\mathbf{p}^N))\int \mathrm{d}^{3N}\mathbf{r}^N\,\exp(-\beta\mathcal{V}(\mathbf{r}^N))\\ &= f(N)\int\prod_{i=1}^{N}\mathrm{d}^3\mathbf{r}_i\,\exp\left(-\frac{\beta\mathbf{p}_i^2}{2m}\right)\int \mathrm{d}^{3N}\mathbf{r}^N\,\exp(-\beta\mathcal{V}(\mathbf{r}^N))\\ &=: \frac{1}{N!\Lambda^{3N}}Z_N\,,\end{aligned} \tag{1.60}$$

where $\Lambda = h/\sqrt{2\pi m k_B T}$ is the thermal wavelength and we have defined the *configuration integral* to be

$$Z_N = \int \mathrm{d}^{3N}\mathbf{r}^N\,\exp(-\beta\mathcal{V}(\mathbf{r}^N))\,. \tag{1.61}$$

This is the more interesting quantity. For example, if we want to know the probability distribution $P_N(\mathbf{r}^N)$ for the configuration of the system, then we need to evaluate

$$P_N(\mathbf{r}^N) = \frac{\exp(-\beta\mathcal{V}(\mathbf{r}^N))}{Z_N}\,. \tag{1.62}$$

The factor Λ^{3N} in the partition function, absorbing the h^{3N}, can be seen as a temperature dependent version of the volume element in the configuration space. The deeper significant of Λ is that it provides a criterion for the approach from the quantum to the classical limit. Quantum effects can be ignored in equilibrium statistics if Λ is smaller than any characteristic length in the system.

1.3 Temperature in Molecular Dynamics

Temperature was introduced in 1.51 as a parameter in the canonical ensemble, and via the fundamental equation (1.57), this statistical mechanical temperature is identified with the empirical temperature in classical thermodynamics. It is not immediately obvious, however, how to define and measure temperature in a MD simulation. To do this, we have to return to the microcanonical ensemble and find an observable (and correspondingly a phase function) whose microcanonical expectation value is a simple function of temperature, preferably linear. This would then allow us to measure the temperature of the ensemble by tracking the time average of the phase function over a sufficiently long period by the ergodic hypothesis. Such phase function is the kinetic energy, whose canonical average is

$$K = \left\langle\sum_{i=1}^{N}\frac{\mathbf{p}_i^2}{2m_i}\right\rangle_{NVT} = \frac{3}{2}Nk_BT \tag{1.63}$$

in three dimensional system, as given by the equipartition theorem. The microcanonical average $\langle - \rangle_{NVE}$ (1.45) and the canonical average $\langle - \rangle_{NVT}$ (1.54) are not identical in general. But in Part II Statistical Mechanics we have shown that such fractional difference is vanishing as $N \to \infty$ — all ensembles are equivalent in the thermodynamic limit. Therefore the microcanonical average of the kinetic energy of a many particle system will also approach $\frac{3}{2}Nk_BT$. Hence we can define an instantaneous or kinetic temperature function $\mathcal{T}$ in terms of the instantaneous kinetic energy $\mathcal{K}$ via

$$\mathcal{T} = \frac{1}{3k_B T} \sum_{i=1}^{N} m_i \mathbf{v}_i^2 = \frac{2}{3k_B N} \mathcal{K} \,, \tag{1.64}$$

which, averaged over a MD run over a long time will give us the temperature of a system

$$T = \frac{1}{M} \sum_{i=1}^{M} \mathcal{T}(t_m) \,. \tag{1.65}$$

1.3.1 Velocity Rescaling

Having found a method of measuring temperature in a MD run, the next problem is how to impose a specified temperature on the system control it during a simulation. Several approaches has been developed, a the most simple one of them is just to scale all particle velocities by a factor determined from the current instantaneous temperature and desired temperature. Suppose the current instantaneous temperature $T(t)$ is considerably different from our desired target temperature, and we want to adjust it to T_0. Then we only need to rescale all current velocities $\mathbf{v}_i$ to

$$\mathbf{v}_i' = \sqrt{\frac{T_0}{T}} \mathbf{v}_i = \sqrt{\frac{K_0}{\mathcal{K}(\mathbf{x}^N(t), \mathbf{p}^N(t))}} \mathbf{v}_i \,. \tag{1.66}$$

In the canonical ensemble, velocities are distributed according to a Gaussian, leading to the famous Maxwell–Boltzmann distributions. The probability functions for each of the three Cartesian components of velocity of every particle i is strictly a Gaussian

$$P(v_{x,i}) = \sqrt{\frac{m_i}{2\pi k_B T}} \exp\left(-\frac{m_i v_{x,i}^2}{2k_B T}\right) \,, \tag{1.67}$$

and the same for $v_{y,i}$ and $v_{z,i}$. Temperature rescaling only alters the width of the velocity distribution — it will not change a non-equilibrium distribution (non-Gaussian) into a Gaussian. Due to the chaotic motion of particles, the velocity distribution should eventually converge to a Gaussian, although it may take a while for this to establish.

We can accelerate this equilibration process by interfering with the dynamics more strongly and randomise the velocities by a sampling from a Gaussian distribution — the *thermostats* described in the next section are one approach to do this.

1.3.2 Thermostats

The simple velocity scaling has an apparent advantage of interfering the dynamics minimally by only scaling the velocities and not changing anything else. However, in principle this action is not what a canonical ensemble (or any standard ensemble) does to keep the temperature of a system constant. In addition, this algorithm can produce artifacts when frequently applied because energy will be transferred from other modes to the translational and rotational degrees of freedom — the system acquires high linear momentum and experiences extremely damped internal motions, being frozen into a single conformation, reminiscent of an ice cube flying through space, leading to a so called *flying ice cube* effect. This is wholly unphysical, since it violates the principle of equipartition of energy, which states that the energy should be equally partitioned into every degree of freedom of the molecule.

This problem is solved by using a *thermostat*, which simulates the effect of placing our small simulation system in contact with a infinite heat bath. From the statistical mechanical point of view, this exactly produces a canonical ensemble. There are multiple ways of achieving this, and the approaches can be broadly classified as being stochastic or deterministic. We will focus on stochastic thermostats.

Stochastic thermostats act by adding random noise to the system, which mimic the effect coupling with the heat bath. This will ensure that all accessible constant-energy surface are each visited according to their Boltzmann weight. Although this produces an exact canonical distribution, it comes at the expense of interfering with the dynamics, and so transport properties like diffusion will be affected. If those are of interest then the deterministic thermostat will be better.

Andersen Thermostat

The Andersen method mimics the effect of a heat bath by selecting a certain fraction of the particles/atoms at a regular interval to undergo "collisions" with a heat bath. These collisions are characterised by a collision frequency ν. For discrete time steps of length δt, the probability of a particle undergoing a collision is therefore $\nu\delta t$.

To implement this, we just need to randomly select particles for collision with probability $\nu\delta t$ at each time step, and reassign the velocity of the selected particles from a Maxwell–Boltzmann distribution with desired temperature. By doing so, the velocities after collisions are clearly completely uncorrelated with those before, so this procedure will strongly affect the dynamics if the collision frequency is high.

The Andersen thermostat is useful for sampling conformational space, but not so much for the computation of time-dependent properties.

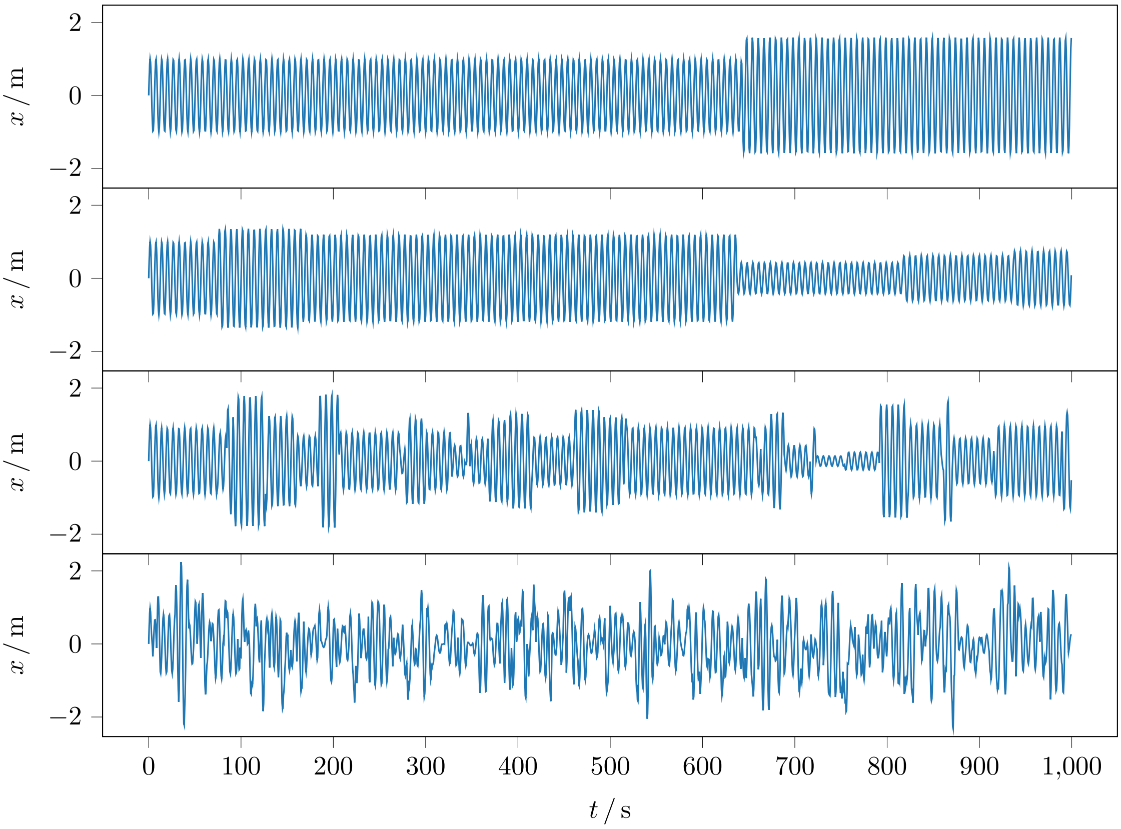

Figure 6: Displacements and velocities of a harmonic oscillation with Andersen thermostats of $\nu = 0.0005, 0.005, 0.05$ and 0.5 respectively.

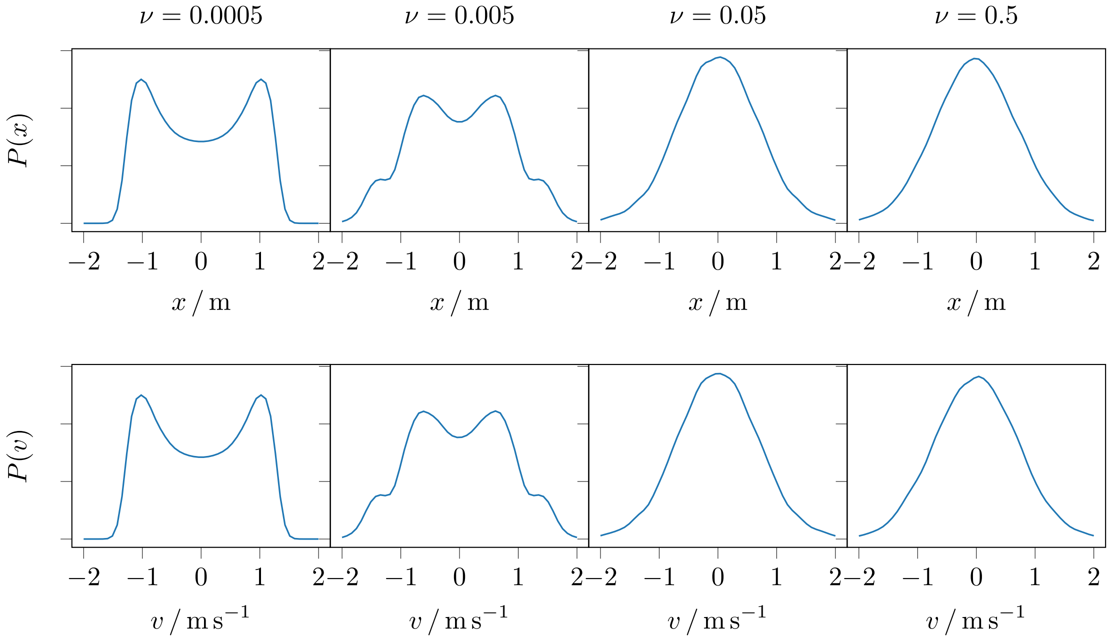

Figure 7: Distributions of displacements and velocities of a harmonic oscillation with Andersen thermostats of different ν.

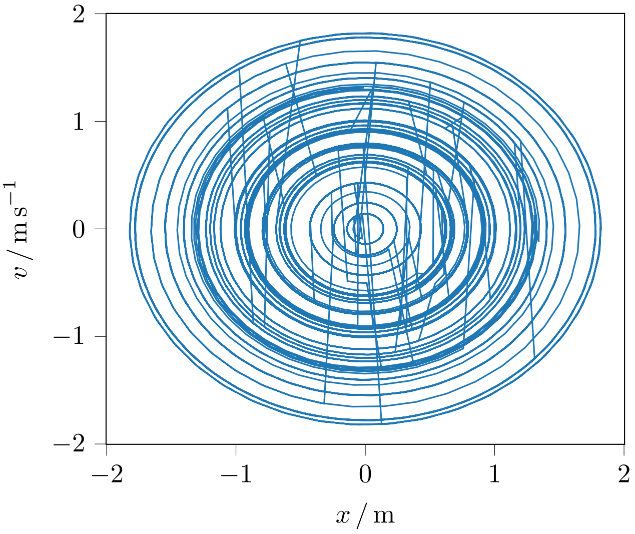

Figure 8: Phase diagram of a harmonic oscillation with Andersen thermostat of $\nu = 0.05$. At this thermalisation frequency, the dynamical nature of harmonic oscillator is not lost while maintaining an efficient thermalisation such that a large area of phase space is explored according to their Boltzmann weight.

Canonical Velocity Rescaling (Non-examinable)

Is is possible to somehow combine the advantages of the fairly continuous trajectory afforded by the velocity rescaling with the canonical sampling we desire in Andersen thermostat? The problem with velocity rescaling is that it will give the correct average kinetic energy by construction, but not necessarily the canonical distribution of kinetic energies. A simple way to fix this is to rescale to match not the average kinetic energy, but a kinetic energy chosen at random from the canonical distribution, given by

$$p(K)\mathrm{d}K = AK^{3N/2-1}\exp(-\beta K)\mathrm{d}K\,, \tag{1.68}$$

where te factor $K^{3N/2-1}$ comes from the volume element in the velocity hyperspace corresponding to the kinetic energy K, and A is a normalisation constant given in this case by

$$A = \frac{1}{\beta^{3N/2}\Gamma(\frac{3N}{2})}\,. \tag{1.69}$$

In one dimension, this is more or less the same as the Andersen thermostat. However, in higher dimensions, the width of the kinetic energy distribution is relatively narrow, so the rescaling will generally be close to unity.

Berendsen Thermostat (Non-examinable)

Instead of abruptly rescaling the temperature at a single time step, Berendsen thermostat rescales the temperature by a exponential relaxation

$$\frac{\mathrm{d}T(t)}{\mathrm{d}t} = \frac{T_0 - T(t)}{\tau}\,, \tag{1.70}$$

where T_0 is the desired temperature and τ is the characteristic time scale of relaxation. This leads to a temperature change of

$$\frac{\delta T}{T_0} = \left[1 - \frac{T(t)}{T_0}\right]\frac{\delta t}{\tau} \tag{1.71}$$

per step. This, however, still does not generate the correct kinetic energy distribution, and can lead to serious artifacts. The stochastic terms introduced by Bussi *et al.* fix this problem. It submit the target temperature to a stochastic differential equation

$$\frac{\delta T}{T_0} = \left[1 - \frac{T(t)}{T_0}\right]\frac{\delta t}{\tau} - 2\sqrt{\frac{T(t)}{3T_0 N\tau}}\xi(t)\,, \tag{1.72}$$

where an extra stochastic term is added.

Nosé–Hoover Thermostat (Non-examinable)

Finally, let's briefly introduce a deterministic thermostat. It couples the system to a heat-bath "particle" with math Q, generalised coordinate s and conjugate momentum p_s, giving what is known as the *Nosé Hamiltonian*

$$\mathcal{H}_N = \sum_{i=1}^{N}\frac{\mathbf{p}_i^2}{2m_i s^2} + U(\mathbf{r}^N) + \frac{p_s^2}{2Q} + gk_B T f(s)\,, \tag{1.73}$$

where g and $f(s)$ are chosen such that the NVE distribution function for the super-system (including the heat bath) corresponds to a canonical distribution function for the physical subsystem. To do this, we start by calculating the phase-space volume for a given total energy E:

$$\Omega \propto \int \mathrm{d}^{3N}\mathbf{r}^N\,\mathrm{d}^{3N}\mathbf{p}^N\,\mathrm{d}s\,\mathrm{d}p_s\,\delta\left(\sum_{i=1}^{N}\frac{\mathbf{p}_i^2}{2m_i s^2} + U(\mathbf{r}^N) + \frac{p_s^2}{2Q} + gk_B T f(s) - E\right)\,. \tag{1.74}$$

We can recover the physical Hamiltonian

$$\mathcal{H}(\mathbf{r}^N, \mathbf{p}^N) = \sum_{i=1}^{N}\frac{\mathbf{p}_i}{2m_i} + U(\mathbf{r}^N) \tag{1.75}$$

by scaling the momentum by $\mathbf{p}_i \to \mathbf{p}_i/s$, giving

$$\Omega \propto \int \mathrm{d}^{3N}\mathbf{r}^N \, \mathrm{d}^{3N}\mathbf{p}^N \, \mathrm{d}s \, \mathrm{d}p_s \, s^{dN} \delta\left(\mathcal{H}(\mathbf{r}^N, \mathbf{p}^N) + \frac{p_s^2}{2Q} + gk_BTf(s) - E\right) , \tag{1.76}$$

where d is the dimension of the system. We need to find a way to integrate over the heat-bath coordinates s and p_s. Assuming that the argument of the delta function has a single root at $s = s_0$, then we can rewrite

$$\delta(h(s)) = \frac{\delta(s - s_0)}{|h'(s_0)|} , \tag{1.77}$$

and so

$$\Omega \propto \int \mathrm{d}^{3N}\mathbf{r}^N \, \mathrm{d}^{3N}\mathbf{p}^N \, \mathrm{d}p_s \, \frac{s_0^{dN}}{|h'(s_0)|} . \tag{1.78}$$

We would like to choose $f(s)$ and g such that

$$\frac{s_0^{dN}}{|h'(s_0)|} \sim \exp\left(-\frac{\mathcal{H}(\mathbf{r}^N, \mathbf{p}^N)}{k_BT}\right) . \tag{1.79}$$

It turns out that this can be achieved via $f(s) = \ln(s)$ and $g = dN + 1$, giving

$$s_0 = \exp\left(\frac{E - \mathcal{H}(\mathbf{r}^N, \mathbf{p}^N) - \frac{p_s^2}{2Q}}{gk_BT}\right) \tag{1.80}$$

$$\frac{1}{|h'(s_0)|} = \frac{1}{gk_BT} \exp\left(\frac{E - \mathcal{H}(\mathbf{r}^N, \mathbf{p}^N) - \frac{p_s^2}{2Q}}{gk_BT}\right) . \tag{1.81}$$

By doing so, an integration over p_s finally leads to

$$\Omega \propto \frac{\exp\left(\frac{E}{k_BT}\right)\sqrt{2\pi Q k_BT}}{(dN + 1)k_BT} \int \mathrm{d}^{3N}\mathbf{p}^N \, \mathrm{d}^{3N}\mathbf{r}^N \, \exp\left(-\frac{\mathcal{H}(\mathbf{r}^N, \mathbf{p}^N)}{k_BT}\right) , \tag{1.82}$$

proportional to the canonical distribution. A molecular dynamics NVE simulation with the Hamiltonian $\mathcal{H}_N$ should therefore produce a canonical distribution of $(\mathbf{r}^N, \mathbf{p}^N)$ with Hamiltonian $\mathcal{H}$! The equations of motion can be obtained using Hamilton's equation from classical mechanics.

$$\dot{\mathbf{p}}_i = -\frac{\partial H_N}{\partial \mathbf{r}_i} = \mathbf{f}_i \qquad \dot{\mathbf{r}}_i = \frac{H_N}{\mathbf{p}_i} = \frac{\mathbf{p}_i}{m_s s^2} \tag{1.83}$$

$$\dot{p}_s = -\frac{\partial H_N}{\partial s} = \frac{1}{s}\left[\sum_{i=1}^{N} \frac{\mathbf{p}_i^2}{m_i s^2} - gk_BT\right] \qquad \dot{s} = \frac{\partial H_N}{\partial p_s} = \frac{p_s}{Q} . \tag{1.84}$$

The equations are, however, not straightforward to implement numerically. Hoover applied a non-canonical transformation to recast these equations into a more amenable form, known as the *Nosé–Hoover equations.*

Algorithm 1.9 (Nosé–Hoover equations).

$$\dot{\mathbf{p}}_i = \mathbf{f}_i - \frac{p_\eta}{Q}\mathbf{p}_i \qquad \dot{\mathbf{r}}_i = \frac{\mathbf{p}_i}{m_i} \tag{1.85}$$

$$\dot{p}_\eta = \sum_{i=1}^{N} \frac{\mathbf{p}_i^2}{m_i} - dNk_BT \qquad \dot{\eta} = \frac{p_\eta}{Q} . \tag{1.86}$$

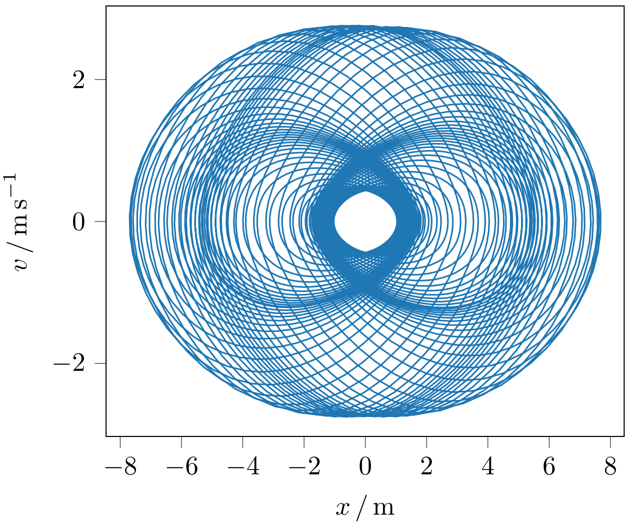

Figure 9: Phase diagram of a harmonic oscillator with Nosé–Hoover thermostat.

1.4 Pressure in Molecular Dynamics

Experiments are most often performed at constant pressure, rendering the NPT (isothermal-isobaric) ensemble the most realistic choice. Especially during the initial equilibration, pressure coupling is essential in order to let the volume of the simulation cell adjust.

We first need a expression for the pressure. The macroscopic pressure can be derived from the free energy, and hence from the bridge relation (1.57), we get

$$\begin{aligned} P &= -\left(\frac{\partial A}{\partial V}\right)_{N,T} = k_B T\left(\frac{\partial \ln Q}{\partial V}\right)_{N,T} \\ &= \frac{k_B T}{Z}\left(\frac{\partial Z}{\partial V}\right)_{N,T}, \end{aligned} \tag{1.87}$$

where

$$Z(N,V,T) = \int \mathrm{d}^{3N}\mathbf{r}^N \, \exp(-\beta\mathcal{U}(\mathbf{r}^N)) \tag{1.88}$$

is the configuration integral. To take differential with respect to V, we switch to the scaled coordinate defined as

$$\mathbf{s}^N = \frac{1}{L}\mathbf{r}^N = V^{-1/3}\mathbf{r}^N\,, \tag{1.89}$$

and so

$$Z(N,V,T) = V^N \int \mathrm{d}^{3N}\mathbf{s}^N \, \exp\left[-\beta\mathcal{U}(V^{1/3}\mathbf{s}_1,\ldots,V^{1/3}\mathbf{s}_N)\right]. \tag{1.90}$$

Differentiate with respect to V gives

$$\frac{\partial Z}{\partial V} = \frac{N}{V}Z(N,V,T) - \beta\int \mathrm{d}^{3N}\mathbf{s}^N \left[\frac{1}{3V}\sum_{i=1}^{N}\mathbf{r}_i\cdot\frac{\partial\mathcal{U}}{\partial\mathbf{r}_i} - \frac{\partial\mathcal{U}}{\partial V}\right]\exp(-\beta\mathcal{U}(\mathbf{r}^N)) \tag{1.91}$$

and so

$$\begin{aligned} P &= \frac{k_B T N}{V} + \frac{1}{3V}\left\langle\sum_{i=1}^{N}\mathbf{r}_i\cdot\mathbf{f}_i\right\rangle \\ &= \frac{1}{3V}\left\langle\sum_{i=1}^{N}\left[\frac{\mathbf{p}_i^2}{m_i} + \mathbf{r}_i\cdot\mathbf{f}_i\right]\right\rangle. \end{aligned} \tag{1.92}$$

From this expression of the ensemble average of pressure, we get an expression of the *isotropic instantaneous pressure*

$$\mathcal{P} = \frac{1}{3V}\sum_{i=1}^{N}\left[\frac{\mathbf{p}_i^2}{m_i} + \mathbf{r}_i \cdot \mathbf{f}_i\right] \tag{1.93}$$

The quantity

$$\mathcal{W} := \sum_{i=1}^{N} \mathbf{v}_i \cdot \mathbf{f}_i \tag{1.94}$$

is also known as the *virial* of the system, and hence the pressure can also be compactly denoted as

$$\mathcal{P} = \frac{1}{3V}\left(2\mathcal{K} + \mathcal{W}\right) . \tag{1.95}$$

1.4.1 Barostats

As for simulating a canonical ensemble using thermostats, we can simulate a isothermal-isobaric ensemble using a *barostat.* If the pressure coupling is only important during the initial equilibrium phase, it can be acceptable to use the simple Berendsen barostat, which imposes the correct external pressure P_0, but violates the thermodynamic ensemble as it has no correct fluctuations. Similar to Berendsen thermostat, it is also a exponential relation

$$\frac{\mathrm{d}P(t)}{\mathrm{d}t} = \frac{P_0 - P(t)}{t} . \tag{1.96}$$

This is achieved via an isotropic scaling factor μ applied to all particle coordinates as well as simulation-cell dimensions

$$\mu = 1 - \frac{\beta\delta t}{3\tau}(P_0 - P) , \tag{1.97}$$

where the β here is the compressibility.

There are also Nosé–Hoover type barostat, in which coordinates, momenta and volume are coupled to a barostat coordinate ϵ via

$$\dot{\mathbf{r}}_i = \frac{\mathbf{p}_i}{m_i} + \underbrace{\frac{p_\epsilon}{W}\mathbf{r}_i}_{\text{barostat}} \qquad \dot{\mathbf{p}}_i = \mathbf{f}_i \underbrace{- \left(1 + \frac{\mathrm{d}}{\mathrm{d}N}\right)\frac{p_\epsilon}{W}\mathbf{p}_i}_{\text{barostat}} \underbrace{- \frac{p_{\eta,1}}{Q_1}\mathbf{p}_i}_{\substack{\text{thermostat}\\ \text{chain}}} . \tag{1.98}$$

In addition, grand canonical ensemble can also be realised using an extended Lagrangian formalism

$$\begin{aligned} L_{\nu VT} = & \sum_{i=1}^{N}\sum_{\alpha}\frac{1}{2}ms^2\dot{x}_{i,\alpha}^2 - \sum_{i}\sum_{j\neq i, j\neq f} U_{ij} \\ & \underbrace{+(\nu - N)\left[\frac{1}{2}ms^2\sum_{\alpha}\dot{x}_{f,\alpha}^2 - \sum_{i\neq f} U_{if}\right] + \frac{1}{2}W\dot{\nu}^2 + U_\nu}_{\text{particle bath}} \\ & \underbrace{+\frac{1}{2}Q\dot{s}^2 - U_s}_{\text{heat bath}} , \end{aligned} \tag{1.99}$$

in which

$$U_s = gk_BT\ln(s) \tag{1.100}$$

$$U_\nu = \nu\mu = \nu(\mu_{\text{id}} + \mu_{\text{ex}}) . \tag{1.101}$$

However, this scheme is rarely used in practise due to its complexity. Monte Carlo (see later) is much more convenient for this purpose.

1.5 Condensed Phase Simulations in Practise

In this section, we will discuss some practical aspects of molecular dynamics simulations using condensed phase fluid (e.g. liquid argon) as an example. What is so special about liquids? Unlike solids the atoms in liquid have no fixed equilibrium position, so there is no *long range order* in the form of a lattice. This is true for gases as well, but unlike gases, the particle density in liquid is high, often comparable with corresponding solid. The atoms in liquids are strongly interacting, establishing a local environment very similar to solids. Liquids exhibit solid-like *short range order.*

Under Born–Oppenheimer approximation, we can write the potential energy as a function of the nuclear positions only

$$U = U(\mathbf{r}_1, \ldots, \mathbf{r}_N) = U(\mathbf{r}^N)\,, \tag{1.102}$$

and then the force acting on particle i given a nuclear configuration $\mathbf{r}^N$ is

$$\mathbf{f}_i(\mathbf{r}^N) = -\frac{\partial U(\mathbf{r}^N)}{\partial \mathbf{r}_i} = m_i \ddot{\mathbf{r}}_i\,. \tag{1.103}$$

We can then try to partition the Born–Oppenheimer potential energy surface onto many-body terms

$$U(\mathbf{r}^N) = \sum_i U_1(\mathbf{r}_i) + \sum_{i,j>i} U_2(\mathbf{r}_i, \mathbf{r}_j) + \sum_{i,j>i,k>j} U_3(\mathbf{r}_i, \mathbf{r}_j, \mathbf{r}_k) + \ldots \tag{1.104}$$

We can ignore the one-body term because it will be constant if the space is homogenous, as this term will be a constant. Three-body interactions and above are usually due to polarisations, and accounts for $\sim 10\%$ to the total interactions in liquid argons. This percentage may be higher for more polarisable systems. If we are assuming interactions are pairwise additive, then we are also ignoring three-body interactions and higher, so we are only left with two-body (pairwise) interactions.

1.5.1 Lennard–Jones Potential

A first step is to choose what model of interaction do we use. A simple example is the Lennard-Jones potential

$$V(\mathbf{r}) = 4\epsilon \left[\left(\frac{\sigma}{r}\right)^{12} - \left(\frac{\sigma}{r}\right)^{6} \right]\,. \tag{1.105}$$

It has a long range r^{-6} attractive force to account for the van der Waals dispersion, and a short range r^{-12} repulsive force due to electron density overlap. For argon, $\sigma \approx 3.4\,\text{Å}$ and $\epsilon \approx 1.65 \times 10^{-21}\,\text{J}$. This also allows us to express everything in reduced unit, in which energies, lengths and masses are scaled by $E^* = E/\epsilon$, $r^* = r/\sigma$ and $m^* = m/m_0$, where m_0 is the mass of the particle. Under these definitions, all Lennard–Jones potentials are the same in reduced units

$$V^*(\mathbf{r}) = 4 \left[\left(\frac{1}{r^*}\right)^{12} - \left(\frac{1}{r^*}\right)^{6} \right]\,. \tag{1.106}$$

This also allows us to define other scaled quantities, like scales density $\rho^* = \rho\sigma^3$, scales temperature $T^* = k_B T/\epsilon$, scaled pressure $P^* = P\sigma^3/\epsilon$ and scaled time $t^* = \sqrt{\epsilon/m\sigma^2}t$.

1.5.2 System Size and Periodic Boundary Conditions

Having chosen the force field, we can set up our simulation cells. The thermodynamic state of a liquid is specified by only two parameters, the temperature T and the pressure P, or alternatively the temperature T and the particle number density $\rho = N/V$. This means that if you want to simulate a specific state of the liquid, choosing the system size is equivalent to choosing how many particles you want to put into the cell. Due to the limited computational power, we cannot make the cell as large as we want. In the early days of molecular dynamics, the number of atoms was typically in the order a 100. Due to the rapid progress in the performance of computer hardware, this number is continuously increasing. A simulation of systems consisting of 10^5 atoms are common nowadays.

System size in MD is in practice a compromise between the length scale of the problem of interest and the minimum duration of a run required for proper statistical sampling. If we are interested in, for example, the onset of freezing of the system, then the size of the system must be much larger than if we want to study the distribution of atoms in a stable liquid. Similarly, computations of transport properties, such as diffusion coefficients, will require much longer runs than the estimation of internal energy.

However, a real world system rarely consists of $\sim 10^5$ atoms. There will be significant surface/boundary and some finite size effect if we directly use a small system for simulation. We want the system to mimic a bulk, homogenous liquid or solid. To do this, we can either take a very big cluster and hope that in the interior of the cluster the surface effect can be neglected, or more cleverly, we can use the periodic boundary condition. To do this, we make our simulation cell into a parallelepiped (e.g. simply a cube), and repeat its contents over the whole space, mimicking the homogeneous state of a liquid or solid. If the MD box is spanned by three vectors $\mathbf{a}, \mathbf{b}, \mathbf{c}$ and the cells are displaced by $\ell\mathbf{a} + m\mathbf{b} + n\mathbf{c}$, where $\ell, m, n \in \mathbb{Z}$. This means that if we have a particle in $\mathbf{r}_i$ in the central cell, then there will also be particles at $\mathbf{r}_i + \ell\mathbf{a} + m\mathbf{b} + n\mathbf{c}$ for all $\ell, m, n \in \mathbb{Z}$. This means that we can simulate a infinite system with infinite particles by only calculating the motion of N particles in the central cell.

Still, due to the periodic nature, applying periodic boundary condition to a small cell will still introduce certain errors, called finite size effect. This can be small or rather serious depending on nature of the system. Moreover, note that the linear momentum is still a constant of motion in such a set of infinitely replicated systems. The conservation of angular momentum, however, is lost as a result of the reduction of rotational symmetry from spherical to cubic.

1.5.3 The Minimum Image Convention and Truncation of Interaction

Periodic boundary conditions create some other difficulties. Since the size of the simulation cell is now effectively infinite, a particle will now interact with an infinite number of particles, making the force evaluation difficult. The potential energy of the particles in the central cell, corresponding to $(\ell, m, n) = (0, 0, 0)$, is a sum of the interactions over all cells:

$$\mathcal{V}(\mathbf{r}^N) = \frac{1}{2}\sum_{i}^{N} V_i(\mathbf{r}^N) \tag{1.107}$$

$$V_i(\mathbf{r}^N) = \sum_{\ell,m,n=-\infty}^{\infty} \sum_{j}^{N}{}' V(\|\mathbf{r}_j + \ell\mathbf{a} + m\mathbf{b} + n\mathbf{c} - \mathbf{r}_i\|)\,, \tag{1.108}$$

where the $'$ indicates that we are excluding $j = i$ for $\ell, m, n = 0$ (self interaction in the central cell).

For short range interactions like the van der Waals interaction, it is possible to make the simplification that if the system is sufficiently large, then the contributions of interactions with all images of the same atom, except the nearest, can be disregarded because they are too far away. Notice that the nearest image can be in the same (i.e. central) cell, but it can also be in one of the neighbouring cells if the two particles are more than half a box away in one direction in the central cell. This approximation is known as the *minimum image approximation.* The distance of particle i to the nearest image of particle j can be easily calculated from their positions in the central cell, using

$$\mathbf{r}_{ij}^{\mathrm{MIC}} = \mathbf{r}_j - \mathbf{r}_i - L\,\mathrm{round}\left(\frac{\mathbf{r}_i\mathbf{r}_j}{L}\right)\,. \tag{1.109}$$

One further thing we can do is to truncate the Lennard–Jones potential at some *cutoff* radius.

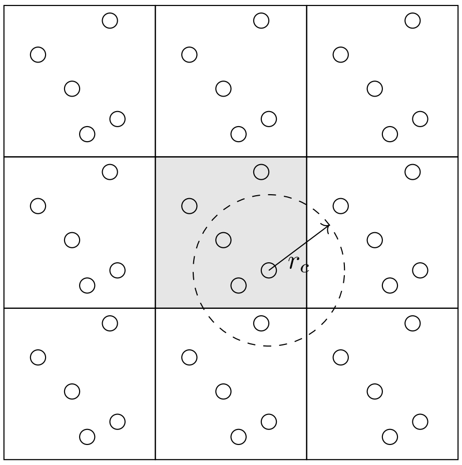

Figure 10: A simulation cell with cyclic boundary condition and cutoff radius $r = r_c$.

This is because such an interaction decays sufficiently quickly: if $r = 3\sigma$, then $V(r) = -0.005\epsilon$. Therefore, we can choose to neglect the contribution to energy and forces beyond this distances. This is done by letting $V_c(r) = 0$ for $r > r_c$, where r_c is the cutoff radius. However, we need to maintain the continuity of the potential, so we need to shift up the potential for $r \leq r_c$ by $|V(r_c)|$. The truncated potential therefore looks like

$$V_c(r) = \begin{cases} V(r) - V(r_c) & r \leq r_c \\ 0 & r > r_c \end{cases}. \tag{1.110}$$

We would often set $r < \frac{L}{2}$ to avoid self-interaction artefact.

1.5.4 Pair Lists

When the cutoff radius r_c is much smaller than the cell dimensions, a lot of time will be spent checking whether a given pair of atoms is within the cutoff, when in fact most lie outside of it. In this case a useful time-saving measure it to use a "pair list" of atoms which are within $r_c + \delta r$ of each other. Provided that this list is updated sufficiently often that no atom will have moved more than the buffer radius δr between updates, only this list of atom pairs needs to be checked at each time step, rather than all possible pairs.

1.5.5 Initialising Positions and Momenta

For most purposes, we want our simulation to get to equilibrium as fast as possible. You can either pre-arrange the particles on a regular lattice, or place them randomly within the simulation cell. However, putting particles randomly can sometimes lead to extreme coordinates (e.g. two molecules are too close to each other / overlapping), and so sometimes a short steepest-descent is required to remove those situations before the simulation has started.

To set up the initial momenta, we can sample randomly from a Gaussian distribution

$$P(v) \propto \exp\left(-\frac{mv^2}{2k_BT}\right) \tag{1.111}$$

for each component of a particle's velocity. However, these randomly generated velocities sometimes give a non-zero total momentum of the system, so we want to correct non-zero velocities of the centre

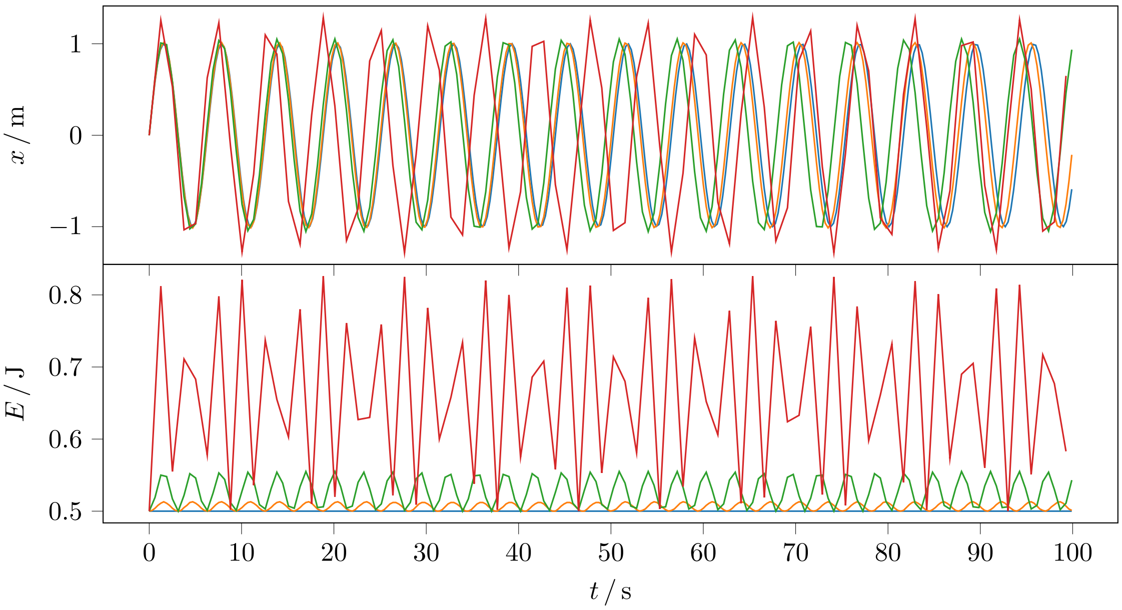

Figure 11: Displacement and energy of a harmonic oscillator using Verlet algorithm with times steps $\delta t = \tau/20$ (orange), $\tau/10$ (green) and $\tau/5$ (red) with exact results (blue).

of mass:

$$\mathbf{v}_{\text{CoM}} = \frac{1}{M} \sum_i m_i \mathbf{v}_i \tag{1.112}$$

$$\mathbf{v}'_i = \mathbf{v}_i - \mathbf{v}_{\text{CoM}} \,. \tag{1.113}$$

Moreover, the randomly generated velocity may deviate from our desired temperature (recall the equipartition theorem), so we need to rescale to velocity by a factor of $\sqrt{T_{\text{target}}/T_{\text{sample}}}$ to reach the desired temperature.

1.5.6 Time Steps

A good choice of time step is a balance between accuracy and computational cost. Too large a time step will lead to large errors in numerical integration. The time step should be significantly smaller than the time scale τ associated with the fastest-frequency oscillation in the system: a step of size $\tau/20$ is usually safe for Verlet-based schemes. The best indication for the breakdown of accuracy in Verlet scheme due to too large time steps is the drift of total energy, which should be rigorously conserved according to Newton's equation of motion.

1.6 Radial Distribution Function

As we commented above, due to the high number density of atoms and strong interactions, liquid often exhibits short range order. This can be captured by the *spatial autocorrelation function*

$$g(\mathbf{r}_1, \mathbf{r}_2) \coloneqq \frac{1}{n_0^2} \langle n(\mathbf{r}_1) n(\mathbf{r}_2) \rangle \tag{1.114}$$

where $n_0 = N/V$ is the average particle density, just like the velocity autocorrelation function you met in Part II Statistical Mechanics. In an isotropic, homogeneous medium, the autocorrelation function

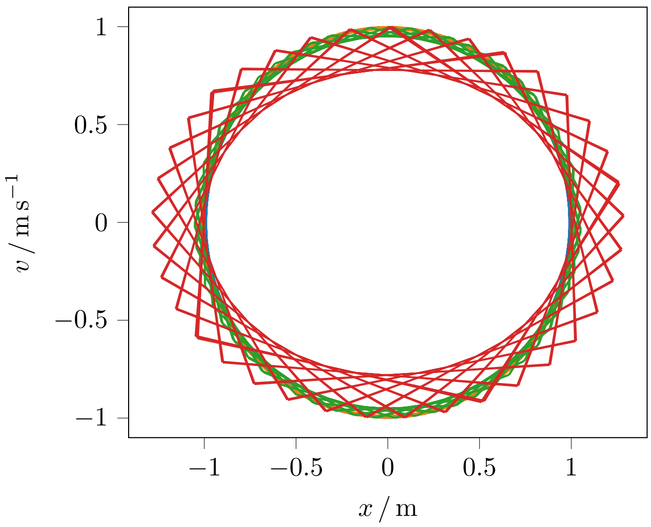

Figure 12: Phase diagram of a harmonic oscillator using Verlet algorithm with times steps $\delta t = \tau/20$ (orange), $\tau/10$ (green) and $\tau/5$ (red) with exact results (blue).

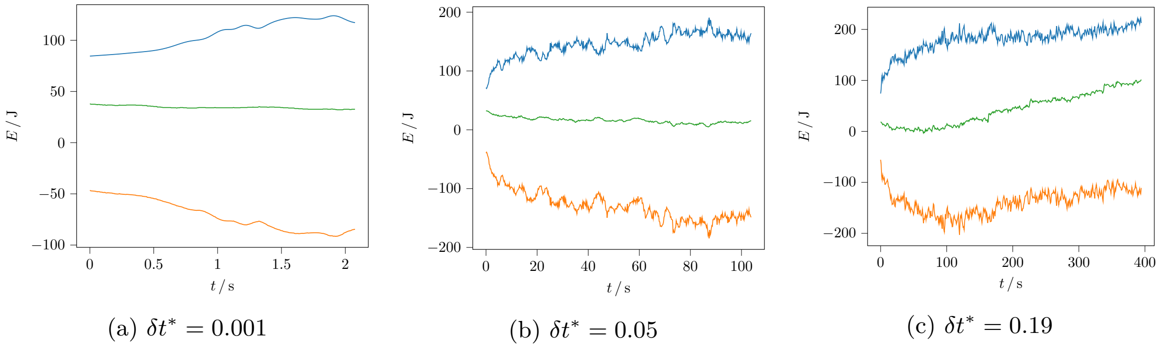

(a) $\delta t^* = 0.001$

(b) $\delta t^* = 0.05$

(c) $\delta t^* = 0.19$

Figure 13: A plot of the computed kinetic energy (blue), potential energy (orange) and total energy (green) of a Lennard-Jones fluid with 100 particles using times steps 0.001, 0.05 and 0.19 in reduced time units. 5000 steps are used for each run. A significant energy drift occurred for $\delta t^* = 0.19$, suggesting that this time step is too large.

should be only dependent on the particle distance $r = \|\mathbf{r}_1 - \mathbf{r}_2\|$, and so it allows us to define the *radial distribution function*

$$g(r) = \frac{n(r)}{n_0}\,. \tag{1.115}$$

This can be understood as a histogram of two-particle distances, which can be constructed by goring through the following steps:

1. Pick a reference particle i at position $\mathbf{r}_i$.
2. Draw a spherical shell of radius r and thickness Δr centred at $\mathbf{r}_i$. Determine the number of particles in the shell, which we denote as $n_i(r, \Delta r)$. A particle j in this shell would satisfy

   $$r \leq \|\mathbf{r}_i - \mathbf{r}_j\| < r + \Delta r\,. \tag{1.116}$$

   A small Δr will give us a high resolution, but it will introduce noises. A large r will smoothen the distribution function, but we may lose some of the structural details.
3. Divide $n_i(r, \Delta r)$ by the volume of the shell to convert it into a number density, and average over reference particles.

   $$\bar{\rho}(r, \Delta r) = \frac{1}{N}\sum_{i=1}^{N}\frac{n_i(r, \Delta r)}{4\pi r^2 \Delta r}\,, \tag{1.117}$$

   where we assumed $\Delta r \ll r$.
4. Normalise this quantity by the particle number density $\rho = N/V$

   $$g(r) = \frac{\bar{\rho}(r, \Delta r)}{\rho} = \frac{V}{4\pi r^2 \Delta r N^2}\sum_{i}^{N} n_i(r, \Delta r)\,. \tag{1.118}$$

   The resulting $g(r)$ is a dimensionless quantity.

A $g(r) > 1$ at some r would mean that we have an enhanced probability of meeting another particle at distance r away from one particle, and $g(r) < 1$ means that there is a depletion region.

A schematic construction of the radial distribution function for a 2D Lennard-Jones fluid is shown in figure 14. For distances $r \ll \sigma$, where σ is the repulsive core diameter, the radial distribution $\to 0$ because particles are excluded from this region. The maximum at a distance little over σ reflects the well defined coordination shell of nearest neighbours around a particle in a liquid. This peak in $g(r)$ is characteristic for the high density prevalent in liquids and is absent in the vapour phase. In most liquids there is also a broader second nearest neighbour peak. As a result of the disorder in liquids, this structure is considerably less pronounced compared to solids. For distances larger than second neighbours, fluctuations gradually takes over and the distribution of atoms becomes homogeneous, with $g(r) \to 1$.

As for a comparison, a crystalline solid has long ranger order extending to infinity, so the radial distribution function should have well defined peaks extending to infinity (ideally) except being broadened by thermal vibrations at non-zero temperatures.

1.6.1 Coordination Numbers

As suggested by figure 14 the integral of the first peak of RDF is related to the average number of particles n_c in the first coordination shell, which is also known as the *coordination number.* In order to measure n_c we must specify how close an atom must approach the central particle in order to be counted as a first neighbour. The position r_{min} of the minimum between the first and second

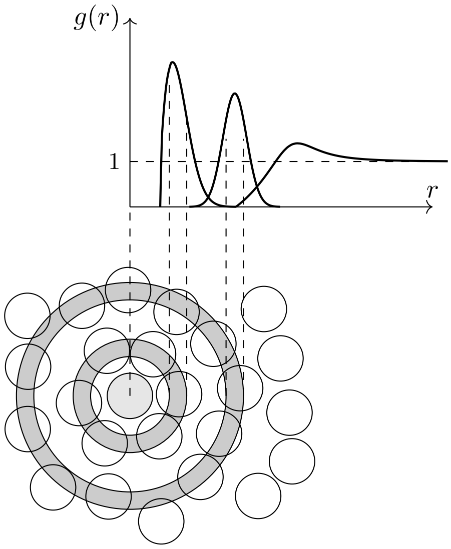

Figure 14: A typical radial distribution function of liquid. $g(r) = 0$ for small r due to hard-core repulsion. There are several peaks with $g(r) > 1$ at intermediate range, corresponding to the first, second and higher coordination shells. At large r, $g(r) \to 1$ as the distribution of particles become decorrelated.

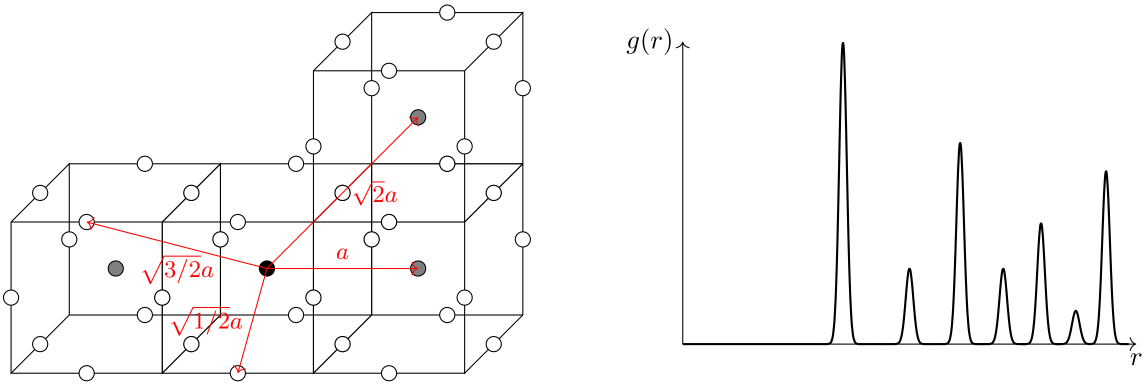

Figure 15: Radial distribution function in a solid fcc crystal.

maximum is used as a common (but not unique) criterion to define the first coordination shell. n_c is then found from the integral (for three dimensional cases)

$$n_c = 4\pi\rho \int_0^{r_c} \mathrm{d}r\, r^2 g(r)\,, \tag{1.119}$$

with $r_c = r_{\min}$ in our cases.

1.6.2 Radial Distribution Function in Statistical Mechanics

The way we introduced the radial distribution function was operational in the sense that it is based on how this quantity is determined in a simulation. We will now give a proper statistical mechanical definition of the radial distribution function making use of the Dirac delta function. We first consider a more general pair correlation function which not only probes the distance r between particles but also the orientation of the displacement vector $\mathbf{r}$.

$$\gamma(\mathbf{r}) = \frac{V}{N(N-1)} \left\langle \sum_{i,j\neq i}^{N} \delta(\mathbf{r}_{ij} - \mathbf{r}) \right\rangle\,, \tag{1.120}$$

where the angular bracket denote an integral over the configurational probability distribution function (1.61). In a more explicit form,

$$\gamma(\mathbf{r}) = \frac{V}{N(N-1)} \sum_{i,j\neq i}^{N} \int \mathrm{d}^{3N}\mathbf{r}^N\, P_N(\mathbf{r}^N)\delta(\mathbf{r}_{ij} - \mathbf{r})\,. \tag{1.121}$$

It is proportional to the probability of observing two particles separated by a vector $\mathbf{r}$. This correlation function with the information on the orientation of $\mathbf{r}$ included is suitable for crystalline solids, in which the lattice defines special directions in space. Liquids are isotropic systems with no preference for a direction, so we expect the function $\gamma(\mathbf{r})$ to depend only on the length $r = \|\mathbf{r}\|$. Using this property, we integrate over a spherical shell $V(r, \Delta t)$ with radius between r and $r + \Delta r$, and assuming that the shell is sufficiently thin, we then write

$$\int_{V(r,\Delta r)} \mathrm{d}^3\mathbf{r}\, \gamma(\mathbf{r}) \approx 4\pi r^2 \Delta r g(r)\,. \tag{1.122}$$

Here the $g(r)$ is the radial distribution function. Substituting the expression of $\gamma(\mathbf{r})$, we get

$$\begin{aligned} g(r) &\approx \frac{V}{4\pi r^2 \Delta r N(N-1)} \int_{V(r,\Delta r)} \mathrm{d}^3\mathbf{r} \sum_{i,j\neq i} \int \mathrm{d}^{3N}\mathbf{r}^N\, P_N(\mathbf{r}^N)\delta(\mathbf{r}_{ij} - \mathbf{r}) \\ &= \frac{V}{4\pi r^2 \Delta r N(N-1)} \int \mathrm{d}^{3N}\mathbf{r}^N\, P_N(\mathbf{r}^N) \sum_{i,j\neq i} \int_{V(r,\Delta r)} \mathrm{d}^3\mathbf{r}\, \delta(\mathbf{r}_{ij} - \mathbf{r})\,, \end{aligned} \tag{1.123}$$

where we have changed the order of integration. The inner integral gives unity when the vector $\mathbf{r}_{ij} = \mathbf{r}_i - \mathbf{r}_j$ lies within volume $V(r, \Delta r)$ and zero otherwise. The delta function therefore counts the number of particle paris with distances between r and $r + \Delta r$. Taking particle i as reference we recover the quantity $n_i(r, \Delta r)$ introduced before

$$n_i(r, \Delta r) = \sum_{j\neq i} \int_{V(r,\Delta r)} \mathrm{d}^3\mathbf{r}\, \delta(\mathbf{r}_{ij} - \mathbf{r})\,. \tag{1.124}$$

Therefore,

$$\begin{aligned} g(r) &\approx \frac{V}{4\pi r^2 \Delta r N(N-1)} \int \mathrm{d}^{3N}\mathbf{r}^N\, P_N(\mathbf{r}^N) \sum_i n_i(r, \Delta r) \\ &= \frac{V}{4\pi r^2 \Delta r N(N-1)} \left\langle \sum_i n_i(r, \Delta r) \right\rangle\,. \end{aligned} \tag{1.125}$$

This becomes an equality in the limit of an infinitely thin shell,

$$g(r) = \lim_{\Delta r \to 0} \frac{V}{4\pi r^2 \Delta r N(N-1)} \left\langle \sum_i n_i(r, \Delta r) \right\rangle . \tag{1.126}$$

Since all particles are equivalent, we must have

$$g(r) = \frac{V}{N-1} \lim_{\Delta r \to 0} \frac{1}{4\pi r^2 \Delta r} \langle n(r, \Delta r) \rangle , \tag{1.127}$$

where we removed the subscript i to indicate a generic particle. We identify this linked to our instantaneous, histogramic radial distribution function (1.118) via

$$g_{\text{stat}}(r) = \frac{N-1}{N} g_{\text{hist}}(r) , \tag{1.128}$$

where $(N-1)/N$ is a good approximation to 1 except at very low density.

Appendices

A Noether's Theorem

The simplest way of deriving the Noether's theorem is to use the Lagrangian mechanics, which is another way of formulating classical mechanics. First let's be clear of our notations. For a system of N particles in d dimensions, we will rewrite the coordinates $\mathbf{r}_i$ as x^A, where $A = 1, \dots, dN$. The Newton's equations are

$$\dot{p}_A = -\frac{\partial V}{\partial x^A}\,, \tag{A.1}$$

where $p_A = m_A \dot{x}^A$. To reduce the cluttering in notations, when we write x^A in the argument of a function, we mean that it is a function of all x^A.

Lagrangian mechanics starts from defining the Lagrangian of a system.

Definition A.1. The *Lagrangian* for a system is defined by

$$L(x^A, \dot{x}^A) = T(\dot{x}^A) - V(x^A)\,, \tag{A.2}$$

where $T = \frac{1}{2}\sum_A m_A(\dot{x}^A)^2$ is the kinetic energy and $V(x^A)$ is the potential energy.

Note the weird minus sign between the kinetic and the potential energy. Despite this strange definition of the Lagrangian, it works really elegantly.

If we know that at $t = t_0$, the particles are at $x^A(t_0) = x_0^A$, and at $t = t_1$, the particles are at $x^A(t_1) = x_1^A$, there are infinite ways the systems can evolve with times between these two end points. How do we find the true paths $x^A(t)$ taken by the particles?

Theorem A.2 (Principle of Least Action). The actual path taken by the system is an extremum of the *action*, defined by

$$S[x^A(t)] = \int_{t_0}^{t_1} \mathrm{d}t\, L(x^A(t), \dot{x}^A(t))\,. \tag{A.3}$$

The S is an example of a *functional.* It maps functions to a number.

Proof. Consider varying a given path slightly, so

$$x^A(t) \longrightarrow x^A(t) + \delta x^A(t)\,, \tag{A.4}$$

where we fix the end points of the path by demanding $\delta x^A(t_0) = \delta x^A(t_1) = 0$. Then this results in a change in the action

$$\delta S = \delta\left[\int_{t_0}^{t_1} \mathrm{d}t\, L\right] \tag{A.5}$$

$$= \int_{t_0}^{t_1} \mathrm{d}t\, \delta L \tag{A.6}$$

$$= \int_{t_0}^{t_1} \mathrm{d}t \sum_A \frac{\partial L}{\partial x^A}\delta x^A + \frac{\partial L}{\partial \dot{x}^A}\delta \dot{x}^A\,. \tag{A.7}$$

We integrate the second term by parts to get

$$\delta S = \int_{t_0}^{t_1} \mathrm{d}t \sum_A \left[\frac{\partial L}{\partial x^A} - \frac{\mathrm{d}}{\mathrm{d}t}\left(\frac{\partial L}{\partial \dot{x}^A}\right)\right]\delta x^A + \left[\frac{\partial L}{\partial \dot{x}^A}\delta x^A\right]_{t_0}^{t_1}\,. \tag{A.8}$$

The boundary term vanishes since we required $\delta x^A(t_0) = \delta x^A(t_1) = 0$. At an extremum of the action S, $\delta S = 0$ for all changes in the path $\delta x^A(t)$. This holds if and only if

$$\frac{\partial L}{\partial x^A} - \frac{\mathrm{d}}{\mathrm{d}t}\left(\frac{\partial L}{\partial \dot{x}^A}\right) = 0\,. \tag{A.9}$$

for all A. This are known as the Euler–Lagrange equations. To finish the proof, we only need to show that Euler–Lagrange equations are equivalent to Newton's equations. From the definition of the Lagrangian, we have

$$\frac{\partial L}{\partial x^A} = -\frac{\partial V}{\partial x^A}\,, \tag{A.10}$$

while

$$\frac{\partial L}{\partial \dot{x}^A} = p_A\,. \tag{A.11}$$

Then it's easy to see that Newton's equations (A.1) are indeed equivalent to Euler–Lagrange equations (A.9). □

In fact Lagrangian mechanics is much more powerful than that. It turns out we can use any generalised coordinate we want (e.g. spherical, hyperbolic, or just some arbitrary parameters that uniquely defines the configuration of the system), and we may add constraints to the coordinates, making it much more powerful than Newton's formulation of classical mechanics. Unfortunately, we can't go into too much of detail here. In you are interested, see e.g. Prof. David Tong's notes on Classical Dynamics. But the important conclusion is that for any Lagrangian written in in generalised coordinates $L(q_i, \dot{q}_i, t)$, the Euler–Lagrange equations still hold:

$$\frac{\partial L}{\partial q_i} - \frac{\mathrm{d}}{\mathrm{d}t}\left(\frac{\partial L}{\partial \dot{q}_i}\right) = 0\,. \tag{A.12}$$

Definition A.3. Consider a one-parameter transformation of maps

$$q_i(t) \longrightarrow Q_i(s,t) \tag{A.13}$$

for $s \in \mathbb{R}$ such that $Q_i(0,t) = q_i(t)$. Then this transformation is said to be a *continuous symmetry* of the Lagrangian L if

$$\frac{\partial}{\partial s} L(Q_i(s,t), \dot{Q}_i(s,t), t) = 0\,. \tag{A.14}$$

Theorem A.4 (Noether's theorem). For each continuous symmetry, there is a conserved quantity.

Proof.

$$\frac{\partial L}{\partial s} = \sum_i \frac{\partial L}{\partial Q_i}\frac{\partial Q_i}{\partial s} + \frac{\partial L}{\partial \dot{Q}_i}\frac{\partial \dot{Q}_i}{\partial x}\,, \tag{A.15}$$

so we have

$$\begin{aligned} 0 = \left.\frac{\partial L}{\partial s}\right|_{s=0} &= \sum_i \left.\frac{\partial L}{\partial q_i}\frac{\partial Q_i}{\partial s}\right|_{s=0} + \left.\frac{\partial L}{\partial \dot{q}_i}\frac{\partial \dot{Q}_i}{\partial x}\right|_{s=0} \\ &= \sum_i \frac{\mathrm{d}}{\mathrm{d}t}\left(\frac{\partial L}{\partial \dot{q}_i}\right)\left.\frac{\partial Q_i}{\partial s}\right|_{s=0} + \left.\frac{\partial L}{\partial \dot{q}_i}\frac{\partial \dot{Q}_i}{\partial s}\right|_{s=0} \\ &= \frac{\mathrm{d}}{\mathrm{d}t}\left(\sum_i \left.\frac{\partial L}{\partial \dot{q}_i}\frac{\partial Q_i}{\partial s}\right|_{s=0}\right)\,. \end{aligned} \tag{A.16}$$

The quantity

$$\sum_i \left.\frac{\partial L}{\partial \dot{q}_i}\frac{\partial Q_i}{\partial s}\right|_{s=0} \tag{A.17}$$

is constant for all time. □

Let's find some examples.

Example. Homogeneity of space.

Consider a system of N particles with Lagrangian

$$L = \frac{1}{2}\sum_i m_i \dot{\mathbf{r}}_i{}^2 - V(r_{ij})\,, \tag{A.18}$$

where $V(r_{ij})$ means that the potential is only dependent on the relative distances $r_{ij} = \|\mathbf{r}_i - \mathbf{r}_j\|$ between particles, not on their absolute positions. Then this Lagrangian has symmetry of translation: $\mathbf{r}_i \to \mathbf{r}_i + s\mathbf{n}$ for any vector $\mathbf{n}$ and real number s.

$$L(\mathbf{r}_i, \dot{\mathbf{r}}_i, t) = L(\mathbf{r}_i + s\mathbf{n}, \dot{\mathbf{r}}_i, t)\,. \tag{A.19}$$

Then by Noether's theorem, the constant that holds in constant is

$$\sum_n \frac{\partial L}{\partial \dot{\mathbf{r}}_i} \cdot \mathbf{n} = \sum_i \mathbf{p}_i \cdot \mathbf{n}\,. \tag{A.20}$$

The component of linear momentum in any direction is conserved, as so

$$\sum_i \mathbf{p}_i \tag{A.21}$$

is also conserved.

Homogeneity in space $\implies$ translational invariance of L $\implies$ conservation of total linear momentum.

Example. Isotropy of Space.

The isotropy of space means that a closed system is invariant under rotations around an axis $\hat{\mathbf{n}}$, so all $\mathbf{r}_i \to \mathbf{r}'_i$ are rotated by the same amount. To work out the corresponding conserved quantity it suffices to work with the infinitesimal form of the rotations

$$\mathbf{r}_i \longrightarrow \mathbf{r}_i + \delta\mathbf{r}_i = \mathbf{r}_i + \alpha\hat{\mathbf{n}} \times \mathbf{r}_i\,, \tag{A.22}$$

where α is infinitesimal. To see that this is indeed a rotation, you can calculate the length of the vector and notice it is preserved to linear order in α. Then we have

$$L(\mathbf{r}_i, \dot{\mathbf{r}}_i) = L(\mathbf{r}_i + \alpha\hat{\mathbf{n}} \times \mathbf{r}_i, \dot{r}_i + \alpha\hat{\mathbf{n}} \times \dot{\mathbf{r}}_i)\,, \tag{A.23}$$

giving us the conserved quantity

$$\sum_i \frac{\partial L}{\partial \dot{\mathbf{r}}_i} \cdot (\hat{\mathbf{n}} \times \mathbf{r}_i) = \sum_i \hat{\mathbf{n}} \cdot (\mathbf{r}_i \times \mathbf{p}_i) = \hat{\mathbf{n}} \cdot \mathbf{L}\,. \tag{A.24}$$

This is the component of the total angular momentum in the direction $\hat{\mathbf{n}}$. Since $\hat{\mathbf{n}}$ is arbitrary, $\mathbf{L}$ is conserved.

Isotropy of space $\implies$ rotational invariance of L $\implies$ conservation of total angular momentum.